ORGANOMETALLICS

Article

pubs.acs.org/Organometallics

ONO Dianionic Pincer-Type Ligand Precursors for the Synthesis of σ,π-Cyclooctenyl Iridium(III) Complexes: Formation Mechanism and Coordination Chemistry

Duc Hanh Nguyen, Ingo Greger, Jesús J. Pérez-Torrente,* M. Victoria Jiménez, F. Javier Modrego, Fernando J. Lahoz, and Luis A. Oro*

Departamento de Química Inorgánica, Instituto de Síntesis Química y Catálisis Homogénea-ISQCH, Facultad de Ciencias, Universidad de Zaragoza-CSIC, C/Pedro Cerbuna, 12, 50009 Zaragoza, Spain

Supporting Information

ABSTRACT: The σ,π-cyclooctenyl iridium(III) pincer compounds [Ir(κ^3-pydc-X)(1-κ-4,5-η-C_8H_{13})] (X = H (**1**), Cl, Br) have been prepared from [Ir(μ-OMe)(cod)]$_2$ and the corresponding 4-substituted pyridine-2,6-dicarboxylic acids (H_2pydc-X) or, alternatively, from their lithium salts (X = H) and [Ir(cod)-($CH_3CN)_2$]PF_6. Deuterium labeling studies in combination with theoretical calculations have shown that formation of **1** involves a metal-mediated proton transfer in the reactive intermediate [Ir(κ^2-Hpydc)(cod)], through the solvent-stabilized hydrido complex [IrH(κ^3-pydc)(cod)(CH_3OH)], followed by olefin insertion. The formation of this hydrido intermediate results from solvent-assisted proton transfer through a hydrogen-bonding network, forming an eight-membered metallacycle. In contrast, reaction of [Ir(μ-OMe)(cod)]$_2$ with iminodiacetic acid derivatives, RN($CH_2COOH)_2$, gave the stable iridium(I) mononuclear [Ir{κ^2-MeN(CH_2COOH)(CH_2COO)}(cod)] (R = Me) complex having a free carboxymethyl group and the tetranuclear complex [Ir_4{κ^4-PhN($CH_2COO)_2$}$_2$(cod)$_4$] (R = Ph) with doubly deprotonated ligands. The molecular structure of the related cyclooctene complex [Ir_4{κ^4-PhN($CH_2COO)_2$}$_2$(coe)$_8$] has been determined by X-ray analysis. Reaction of **1** with monodentate N- and P-donor ligands gave the compounds [Ir(κ^3-pydc)(1-κ-4,5-η-C_8H_{13})(L)] (L = py, $BnNH_2$, PPh_3, PMe_3). Reaction of **1** with the short-bite bis(diphenylphosphino)methane (dppm) afforded the mononuclear **1-dppm**, with an uncoordinated P-donor atom, or the dinuclear complex **1_2-dppm** as a function of the molar ratio used. Similarly, the dinuclear complexes **1_2-dppe** and **1_2-dppp** have been prepared using 1,2-bis(diphenylphosphino)ethane (dppe) and 1,3-bis(diphenylphosphino)propane (dppp) as bridging ligands. The diphosphine-bridged dinuclear assemblies have been obtained as two diastereoisomers in a 1:1 ratio due to the chirality of the mononuclear building block. The single-crystal X-ray structures of **1-py** and **1-dppm** are reported.

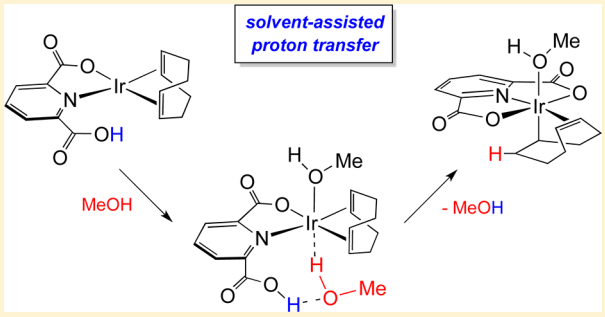

INTRODUCTION

The chemistry of pincer ligands, bearing three coordination sites providing a rigid meridional environment to the metal center, is one of the most dynamic areas in modern inorganic chemistry, due to the impressive number of applications in materials science and catalysis.[1] In spite of the apparent simplicity of the ligand framework, pincer ligands are valuable tools for generating metal complexes with an adequate balance of thermal stability and reactivity. Although a large number of ligands bearing C-, N-, P-, or S-donor-based functionalities have been synthesized,[2] pincer ligands having O-donor fragments have been much less studied.[3] In this context, the ability of OCO and ONO trianionic pincer ligands to support high-oxidation-state metal complexes with vacant coordination sites, which have been recently exploited for a range of catalytic transformations, is remarkable.[4,5]

Low-valent iridium complexes have been reported to show good activity for C−H activation and functionalization processes.[6] Periana et al. have shown that the octahedral Ir(III) complexes [Ir(κ^2-acac)$_2$(R)(py)] (R = CH_3, Ph), bearing two acetylacetonate ligands (acac), one leaving alkyl group, and one accessible coordination site, efficiently catalyzed the hydroarylation of olefins, which likely proceeded via Ir(III)/Ir(V) interconversion.[7] O-donor ligands in these systems play an important role, facilitating the access to high oxidation states by modulating the electron density at the metal centers via a hard/hard interaction or π-donating effects.[8]

Recently, iridium complexes bearing O-based dianionic pincer ligands have attracted considerable attention with regard to C−H bond activation. The robustness and stability of the ligand framework, with strongly electron donating hard oxygen atoms, can provide more facile access to the relatively high oxidation state of the metal center, thereby promoting the C−

Received: August 1, 2013

   dx.doi.org/10.1021/om400767d | *Organometallics* XXXX, XXX, XXX−XXX

H bond oxidative addition under mild conditions. Bercaw and Labinger et al. reported the synthesis of Ir(I) and Ir(III) complexes bearing a diphenolate−imidazolyl−carbene tridentate ligand (Chart 1(i)), but no C−H bond activation

Chart 1. Ligand Framework of O-Based Dianionic Pincer Iridium Complexes (R = ^{t}Bu)

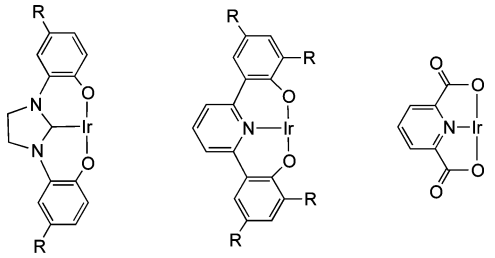

chemistry was demonstrated.[9] Recently, the same group has described the synthesis of bis(phenolate)pyridine iridium(III) pincer complexes (Chart 1(ii)) and their ability to smoothly activate both intra- and intermolecular C−H bonds.[10] On the other hand, at the same time we reported the synthesis of unsaturated iridium(III) pyridinedicarboxylate pincer complexes (Chart 1(iii)), which exhibited a notable catalytic activity in the borylation of arenes involving C−H bond activation under thermal conditions.[11] It is noteworthy that the synthesis of some iridium and rhodium complexes containing pyridine-2,6-dicarboxylate ligands has been described, but no catalytic applications were reported.[12]

In the present contribution we report on the synthesis and reactivity of unsaturated σ,π-cyclooctenyl complexes [Ir(κ^3-pydc-X)(1-κ-4,5-η-C_8H_{13})] (X = H, Cl, Br). The straightforward synthesis of these unusual iridium(III) pincer complexes from pyridine-2,6-dicarboxylic acids and standard dinuclear iridium(I) starting materials, the simple ligand architecture of these complexes, and their potential catalytic applications based on C−H activation have prompted us to investigate their formation mechanism. In addition, the scope of the synthetic methodology for the preparation of iridium(III) pincer complexes derived from related dicarboxylic compounds as precursors has also been investigated.

RESULTS AND DISSCUSION

Synthesis of Pyridinedicarboxylate Pincer Complexes [Ir(κ^3-pydc-X)(1-κ-4,5-η-C_8H_{13})]. The σ,π-cyclooctenyl iridium(III) compound [Ir(κ^3-pydc)(1-κ-4,5-η-C_8H_{13})] (**1**) can be straightforwardly prepared by the reaction of 2,6-pyridinedicarboxylic acid (H_2pydc) with 0.5 molar equiv of the dinuclear 1,5-cyclooctadiene iridium methoxy-bridged complex [Ir(μ-OMe)(cod)]$_2$ in CH_2Cl_2/MeOH at room temperature (method A, Scheme 1). The compound was obtained as the methanol solvate **1**·MeOH, as was confirmed by a X-ray analysis, and isolated as an air- and moisture-stable yellow solid in 90% yield after chromatographic purification.[11] This synthetic method is applicable to the preparation of related 4-substituted pyridine-2,6-dicarboxylate pincer complexes. Thus, reaction of the complex [Ir(μ-OMe)(cod)]$_2$ with 4-chloro- and 4-bromopyridine-2,6-dicarboxylic acids afforded the corresponding complexes [Ir(κ^3-pydc-Cl)(1-κ-4,5-η-C_8H_{13})] (**2**) and [Ir(κ^3-pydc-Br)(1-κ-4,5-η-C_8H_{13})] (**3**), which were isolated as red solids in excellent yield. These complexes are

Scheme 1. Synthetic Routes to [Ir(κ^3-pydc)(1-κ-4,5-η-C_8H_{13})] (1) from 2,6-Pyridinedicarboxylic Acid and Its Lithium Salts[a]

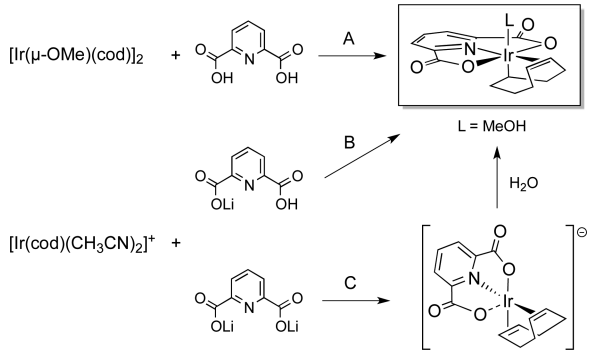

[a]Reactions were conducted in CH_2Cl_2/MeOH (3/1).

scarcely soluble in most organic solvents, including dichloromethane and methanol, although surprisingly the compounds have an acceptable solubility in a 5/1 mixture of both solvents.

The σ,π-cyclooctenyl ligand in complexes **1**−**3** has been unequivocally identified by NMR spectroscopy.[13] For example, the olefinic protons and carbons (=CH) were observed as two characteristic low-field multiplet resonances at 5.87 and 5.64 ppm in the ^{1}H NMR spectrum of **3**, which correlates with those at 89.0 and 85.0 ppm in the ^{13}C{^{1}H} NMR spectrum. The Ir−*C*H resonance was easily identified in the ^{13}C APT spectrum at 14.6 ppm. Full assignment of the resonances and connectivity in the σ,π-cyclooctenyl ligand was achieved with the help of 2D ^{1}H−^{1}H COSY, ^{1}H−^{13}C HSQC, and HMBC experiments.

The stability of **1** allows for alternative synthetic approaches from cationic mononuclear iridium complexes and 2,6-pyridinedicarboxylic acid lithium salts. Thus, treatment of [Ir(cod)(CH_3CN)$_2$]PF_6 with lithium 6-carboxypicolinate (HLi-pydc) in CH_2Cl_2/MeOH gave **1** in 96% yield without the need for chromatographic purification after removing the $LiPF_6$ salt (method B, Scheme 1). It is noteworthy that reaction of [Ir(cod)(CH_3CN)$_2$]PF_6 with lithium pyridine-2,6-dicarboxylate (Li_2pydc) also gave **1** in excellent yield instead of the expected iridium(I) anionic complex Li[Ir(κ^3-pydc)(cod)] (method C, Scheme 1). In this case, the formation of **1** can be explained by the presence of adventitious water in the organic solvents, which plays an important role in providing the required proton for the formation of the cyclooctenyl ligand. In sharp contrast, only a very small amount of **1** was formed on starting from the chlorido-bridged dimer [Ir(μ-Cl)(cod)]$_2$ and pyridine-2,6-dicarboxylate lithium salts, even under heating conditions.

Mechanistic Studies on the Formation of [Ir(κ^3-pydc)(1-κ-4,5-η-C_8H_{13})]. The synthesis of [Ir(κ^3-pydc)(1-κ-4,5-η-C_8H_{13})] (**1**) has been investigated by NMR. First, it is reasonable to propose that the protonation of the methoxido bridges in [Ir(μ-OMe)(cod)]$_2$ by H_2pydc results in the formation of the mononuclear neutral iridium(I) intermediate [Ir(κ^2-Hpydc)(cod)] (**4**) having the monodeprotonated ligand κ^2-N,O coordinated and an uncoordinated carboxyl group (Scheme 1, method A). This species should be also straightforwardly generated by replacement of the labile acetonitrile ligands in [Ir(cod)(CH_3CN)$_2$]$^+$ by lithium 6-carboxypicolinate (Scheme 1, method B). In fact, the clean synthesis of **1** using this method further supports this proposal. The intermediate compound **4**, which is immediately formed after mixing the reagents by both methods, has been

dx.doi.org/10.1021/om400767d | Organometallics XXXX, XXX, XXX−XXX

characterized in solution. The ^{1}H NMR spectrum of [Ir(κ^2-Hpydc)(cod)] (**4**) at 208 K (CD_2Cl_2/CD_3OD) features a set of four resonances at 4.26 and 3.77 ppm (=CH protons) and 2.09 and 1.28 ppm (>CH_2, *exo* and *endo* protons), which is in full agreement with the integrity of the cyclooctadiene ligand. Furthermore, the HR ESI-MS showed peaks at *m*/*z* 490.0633 (ESI+) and 466.0672 (ESI−) corresponding to the ions $[M + Na]^+$ and $[M - H]^-$, respectively. Warming to room temperature resulted in broad resonances, although no evidence of proton transfer from the carboxyl group to the cod ligand was immediately observed. Interestingly, the formation of the related [Ir(κ^2-Hpydc-Br)(cod)] species was also observed under similar conditions.

A plausible mechanism for the proton transfer leading to the cyclooctenyl ligand is a metal-mediated process. Thus, the protonation of the iridium center in [Ir(κ^2-Hpydc)(cod)] (**4**) by the free −COOH arm of the tridentate ligand, formally an oxidative addition, should result in the octahedral iridium(III) hydrido complex [IrH(κ^3-pydc)(cod)]. Subsequent insertion of one of the C=C bonds into the Ir−H bond would account for the formation of **1** (Scheme 2). In this context, it is worth mentioning that the oxidative addition of carboxylic acids to iridium(I) complexes is a well-documented process.[14]

Scheme 2. Proposed Mechanism for the Formation of [Ir(κ^3-pydc)(1-κ-4,5-η-C_8H_{13})(CH_3OH)] (1·MeOH)

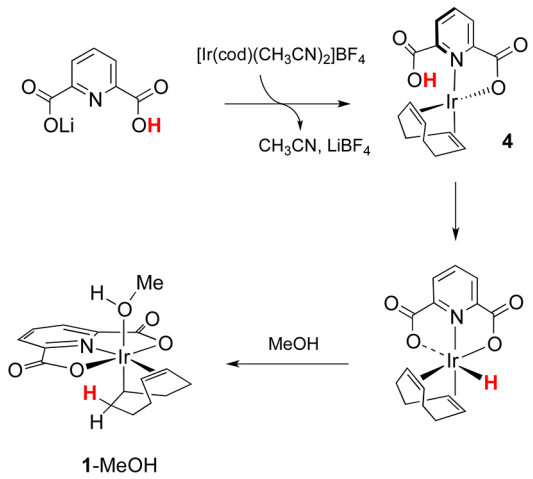

The synthesis of **1** from Li_2pydc, where traces of adventitious water could act as proton source (Scheme 1, method C), requires further comments. Although the reaction of Li_2pydc with H_2O to give back LiHpydc is possible, most probably, the protonation of the carboxylate free arm in the anionic complex Li[Ir(κ^2-pydc)(cod)] by H_2O to give [Ir(κ^2-Hpydc)(cod)] (**4**) and LiOH is taking place. The direct protonation of the iridium center by H_2O in the strongly nucleophilic anionic complex to give a hydrido intermediate is a less likely pathway.[15]

In order to shed light on the operating mechanism for the proton transfer, we have prepared the deuterium-labeled compound [Ir(κ^3-pydc)(1-κ-4,5-η-$C_8H_{12}D$)] (**1-*d*^{1}**) by two different methods. Thus, reaction of $[Ir(cod)(CH_3CN)_2]PF_6$ with lithium pyridine-2,6-dicarboxylate (Li_2pydc) in the presence of D_2O resulted in the complete incorporation of deuterium into the cyclooctenyl ligand (Scheme 1, method C). Interestingly, **1-*d*^{1}** can be also prepared from [Ir(μ-OMe)(cod)]$_2$ and H_2pydc in CD_2Cl_2/CD_3OD (method A). The presence of the $C_8H_{12}D$ cyclooctenyl ligand in **1-*d*^{1}** was confirmed both in the $^{13}C\{^1H\}$ NMR, which showed the expected deuterium-coupled triplet resonance at 34.73 ppm (J_{C-D} = 19.0 Hz), and in the ^{2}H NMR at 1.21 ppm. The *endo* and *exo* protons (8-H) of the resulting >CH_2 next to the Ir−C bond in **1** have been identified at 0.92 (tt, J_{H-H} = 13.9 and 2.2 Hz) and −0.01 ppm (ddd, J_{H-H} = 13.9, 7.3, and 3.6 Hz), respectively (Figure 1a).[11] The triplet feature of the 8-H-*endo* resonance is due to two similarly large couplings with 8-H-*exo* and one of the adjacent H-7 protons with an axial−axial relationship. This assignment is also consistent with the observation that in cyclooctenyl ligands with a metallo-chair conformation the low-shift proton of a geminal pair is located at the face of the cyclooctenyl ligand opposite to the metal fragment.[16] Thus, the lack of a resonance at δ 0.92 ppm in the ^{1}H NMR spectrum of **1-*d*^{1}** (Figure 1b), assigned to the 8-H-*endo* proton, supports the proposed hydride/insertion mechanism, as the migratory insertion proceeds with cis stereochemistry.

Unfortunately, we have not been able to observe any hydrido intermediate by monitoring the reactions leading to complexes **1**−**3**. In addition, the stereochemistry of **1-*d*^{1}** is also compatible with the intramolecular direct protonation of the cyclooctadiene ligand by the carboxyl group. In fact, the direct protonation of cyclooctadiene on electron-rich nickel(0) complexes has been demonstrated.[16] On the other hand, the *exo* nucleophilic attack by methoxide on cyclooctadiene palladium complexes to give chlorido-bridged cyclooctenylmethoxy palladium dimers has been also described.[17]

DFT Calculations on the Proton Transfer Mechanism in [Ir(κ^2-Hpydc)(cod)]. In order to ascertain the proton transfer mechanism in [Ir(κ^2-Hpydc)(cod)] (**4**) leading to the formation of the σ,π-cyclooctenyl iridium(III) compound [Ir(κ^3-pydc)(1-κ-4,5-η-C_8H_{13})] (**1**) as the methanol solvate, **1**·MeOH, a detailed computational study using DFT calculations has been carried out both in the gas phase and in dichloromethane as solvent. In the following discussion energy differences are expressed as ΔG for gas-phase calculations and ΔE (CH_2Cl_2) for solution calculations.

In the gas phase, the optimized structure of the initial intermediate [Ir(κ^2-Hpydc)(cod)] (**4**) shows the expected square-planar coordination environment for an Ir(I) center which is bonded to cod and a κ^2-*N*,*O* coordinated 6-carboxypicolinato ligand. The remaining uncoordinated carboxyl group is located out of the molecular plane and directed away from the iridium center. A prominent feature of the structure of the final Ir(III) reaction product, **1**·MeOH, is that the 2,6-pyridinedicarboxylato ligand plane runs eventually parallel to the unchanged double bond of the σ,π-cyclooctenyl ligand, in a 90° turn relative to the starting position in **4**. This fact, along with the coordination of a methanol molecule to the final complex, suggests some complexity in the reaction mechanism.

Assuming that the reorientation of the tridentate ligand could occur before the proton transfer to the cyclooctadiene ligand, rotation of the 6-carboxypicolinato ligand in **4** and coordination of a MeOH molecule leads to **4a**, which is just 6.8 kcal mol^{-1} above the starting mononuclear complex and has been shown to be a minimum in the potential energy surface of the molecule. The formation of the cyclooctenyl group could proceed by either the formation of a hydrido intermediate followed by insertion of the hydrido ligand into the double bond or by a direct protonation of the double bond by the acidic carboxyl group. Interestingly, the carboxyl group in **4a**

dx.doi.org/10.1021/om400767d | *Organometallics* XXXX, XXX, XXX−XXX

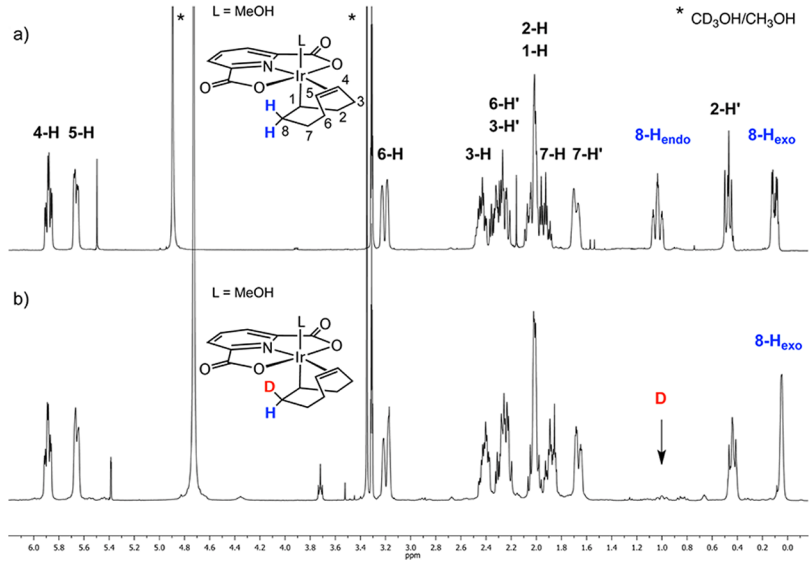

Figure 1. Cyclooctenyl region of the ^{1}H NMR spectra of (a) [Ir(κ^3-pydc)(1-κ-4,5-η-C_8H_{13})] (**1**) and (b) [Ir(κ^3-pydc)(1-κ-4,5-η-C_8H_{12}D)] (**1-*d*^{1}**).

Scheme 3. Gas-Phase DFT Calculated ΔG (in kcal mol^{-1}) Energy Profile for the Proton Transfer Mechanisms in [Ir(κ^2-Hpydc)(cod)] (4) Leading to the Formation of the Methanol Solvate of [Ir(κ^3-pydc)(1-κ-4,5-η-C_8H_{13})] (1)

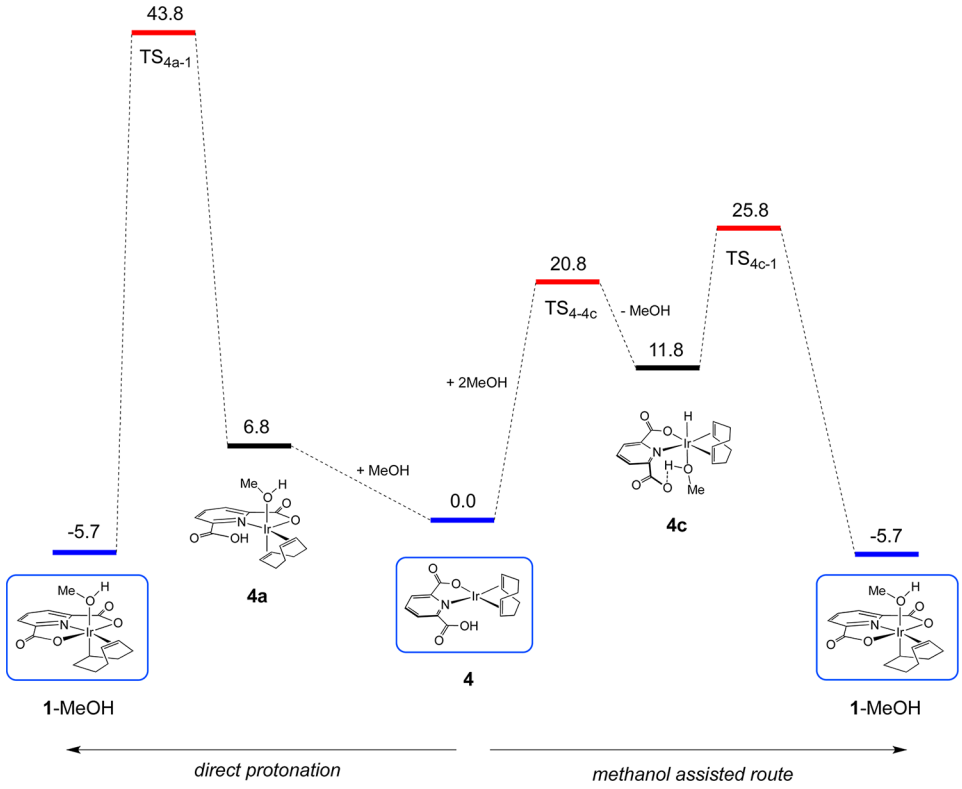

has the required orientation for both processes. Scanning of the Ir−H distance from the carboxyl group in the search for a potential hydrido is always uphill, in the gas phase, and any full optimization reverts to **4a**. On the other hand, scanning the C(olefin)−H distance leads to the transition state $TS_{4a\text{-}1}$ at a relative energy of 37.0 kcal mol^{-1}, which connects with the final complex **1**·MeOH. Although this is a possible reaction pathway, the overall activation energy of 43.8 kcal mol^{-1} from **4** makes it inaccessible (Scheme 3, left side). In solution the computed behavior is somewhat different. It is possible to detect, instead, a transition state leading to the hydrido intermediate **4b** (Figure 2), which eventually leads to the insertion product **1** (see below). Interestingly, the hydrido intermediate **4b** is unstable to a reoptimization in the gas phase, as expected according to the results shown above.

A possible pathway can be provided by participation of alternative hydrido iridium(III) intermediates derived from **4**. The tridentate 2,6-pyridinedicarboxylate ligand can adopt, in principle, either *fac* or a *mer* disposition in an octahedral geometry. The geometry optimization, in the gas phase, of a *fac* mononuclear hydrido isomer leads to the high-energy (25.2 kcal mol^{-1} relative to **4**) and strongly distorted structure **4e**,

dx.doi.org/10.1021/om400767d | *Organometallics* XXXX, XXX, XXX−XXX

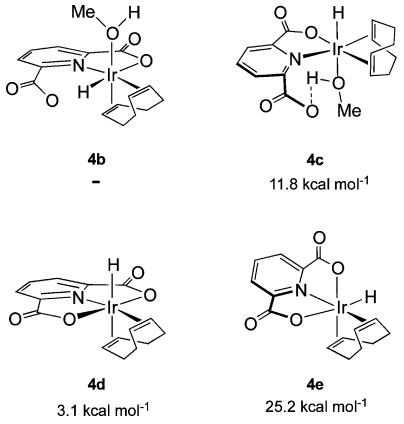

Figure 2. Gas-phase DFT computed energies (ΔG, kcal mol^{-1}) relative to [Ir(κ^2-Hpydc)(cod)] (**4**) for a *mer* (**4d**), *fac* (**4e**), and methanol stabilized (**4c**) isomers of the hydrido complex [IrH(κ^3-pydc)(cod)] (isomer **4b** was found to be stable only in solution calculations).

which shows a pseudooctahedral geometry where the 2,6-pyridinedicarboxylate ligand spans roughly three *fac*-disposed coordination sites in a very strained conformation (Figure 2). This high energy suggests that **4e** is not a viable intermediate. More stable is the pseudooctahedral *mer* hydrido isomer **4d**, where the three donor atoms of the 2,6-pyridinedicarboxylate ligand are coplanar with one of the double bonds of the cyclooctadiene ligand, with the hydrido ligand *trans* to the other double bond of the diolefin, which is very weakly coordinated. In spite of this structure being very close in energy to the starting compound (+3.1 kcal mol^{-1}), it does not have the required stereochemistry to produce the insertion final product. The C═C double bond lies perpendicular to the Ir−H bond, and consequently, the insertion process requires a substantial amount of activation energy, $TS_{4d\text{-}1}$ (33.5 kcal/mol), still too high to be acceptable within the reaction mechanism.

In light of these findings in the gas phase, alternative reaction pathways with explicit participation of methanol have been explored. A more accessible pathway to the insertion process is provided via the hydrido complex **4c**, stabilized by a methanol molecule (Figure 2). This intermediate has lower energy than **4e** (11.8 kcal mol^{-1} relative to **4**) and features a pseudooctahedral coordination geometry with a methanol molecule coordinated (Ir−O, 2.25 Å) *trans* to the hydrido ligand and at hydrogen-bonding distance of an uncoordinated carboxylate group (O···H, 1.45 Å) of the κ^2-N,O coordinated pyridine-2,6-dicarboxylate ligand. The coordination of methanol and the hydrogen bond to the uncoordinated carboxylate group provides relief to the strain observed for the tridentate pyridine-2,6-dicarboxylate ligand in **4e**. In support of the stabilizing role of methanol, calculations of a similar structure using a molecule of THF instead of methanol ends in dissociation of the THF molecule and a hydrido complex with a similar geometry to the strained **4e**. In addition, the formation of the final insertion product bearing a THF ligand instead of methanol, **1**-THF, is just 3.4 kcal mol^{-1} exergonic in contrast to the 5.7 kcal mol^{-1} released in the formation of **1**·MeOH. This is consistent with the very long reaction times required (5 days at room temperature) for the formation of **1** from [Ir(μ-OMe)(cod)]$_2$ and H_2pydc using THF as solvent.

The transition state $TS_{4c\text{-}1}$ located at an activation energy 14 kcal/mol above **4c** (25.8 kcal mol^{-1} global) leads to the insertion product **1**·MeOH (Scheme 3, right side; Figure 3b). Eventually, although this hydrido complex is somewhat less stable than **4d**, it opens a kinetically more feasible reaction pathway. In any case, formation of the intermediate hydrido complexes is endergonic, which agrees with the fact that they remain unobserved during the reaction.

The formation of the hydrido intermediate **4c** from **4** has also been studied. Scanning both the direct and the reverse processes in a search for the corresponding transition structure ends up in the intermediate **4a**. Although the stabilizing role of methanol is required to outline a reasonable reaction pathway to **1**·MeOH, the search of a transition state from **4** to **4c** using just one methanol molecule has been fruitless. The reaction has been studied with two molecules of methanol taking part in the process, one required to account for the coordinated molecule of methanol in the intermediate **4c** and another one as an intervening mediator in the proton transfer of the carboxylic proton to the iridium atom. This has allowed us to find the transition structure TS_{4-4c}, which shows that the process for the formation of the Ir(III) hydrido intermediate takes place by simultaneous transfer of the carboxylic proton to a methanol

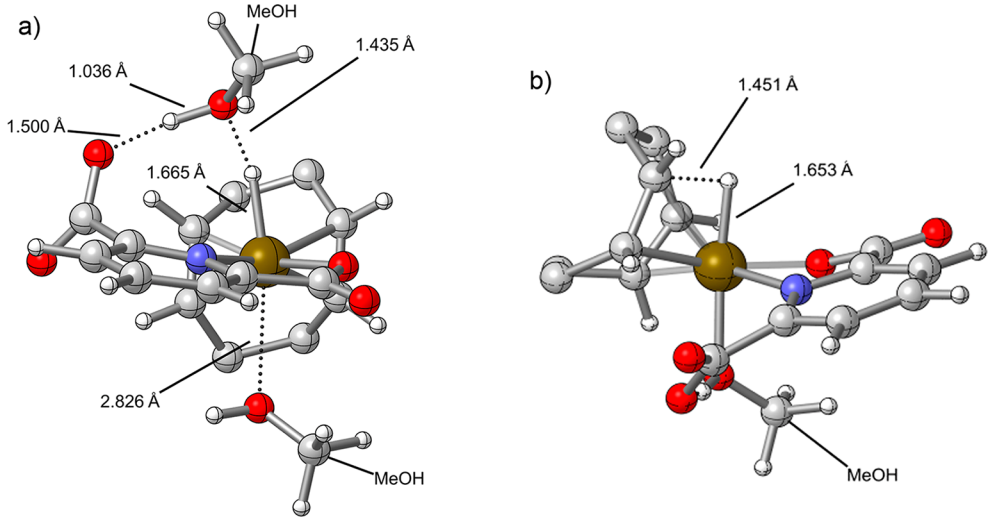

Figure 3. Structures for the transition states TS_{4-4c} (a) and $TS_{4c\text{-}1}$ (b). Some hydrogen atoms have been omitted for clarity.

dx.doi.org/10.1021/om400767d | *Organometallics* XXXX, XXX, XXX−XXX

Scheme 4. DFT Calculated ΔE (in kcal mol^{-1}) Energy Profile in Dichloromethane Solution for the Proton Transfer Mechanisms in [Ir(κ^2-Hpydc)(cod)]·2MeOH (4·2MeOH) Leading to the Formation of the Methanol Solvate of [Ir(κ^3-pydc)(1-κ-4,5-η-C_8H_{13})] (1)

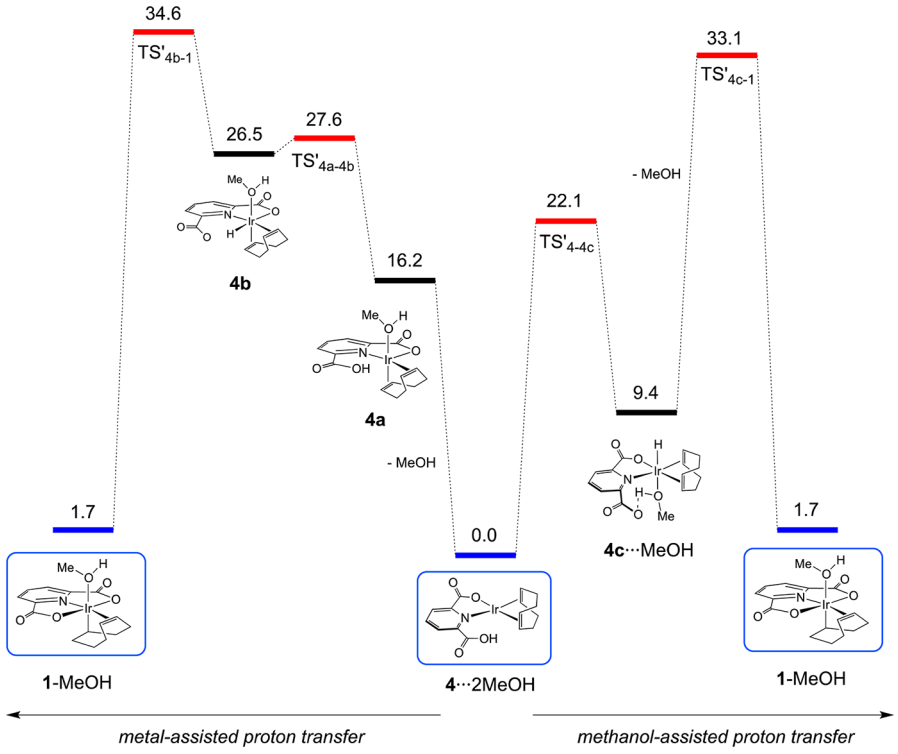

molecule, which transfers its own proton to the iridium center in a concerted way through an eight-membered metallacycle (Figure 3a). The geometry of the transition state is quite advanced toward the formation of the hydrido complex, as there is only 9 kcal/mol of difference between them and its formation is endergonic relative to the starting compound **4**. The distances of the transferred proton between the carboxyl and the methanol are 1.50 Å to the carboxyl oxygen atom and 1.04 Å to the methanol oxygen atom. On the other hand, the hydrido ligand is located 1.66 Å from the iridium atom (1.56 Å in the final product) and 1.43 Å from the methanol oxygen atom. The moderate activation energy (20.8 kcal mol^{-1}) for the proton transfer process along with that involved in the transition from the hydrido complex to the final species (14 kcal mol^{-1}) gives a global activation energy of 25.8 kcal mol^{-1} (Scheme 3, right side), which accounts for the long reaction times required to drive the reaction to completion. Optimization in solution, using dichloromethane as solvent and SMD as solvation model, shows some differences but again illustrates that this is the most accessible pathway to a hydrido intermediate.

In order to trace the solution energy landscape, the TS_{4-4c} and both end products of the IRC calculation were reoptimized in solution, including the two intervening methanol molecules. These calculations have shown a remarkable stabilization in solution of **4** by the two hydrogen-bonded methanol molecules (**4**·2MeOH, 18.0 kcal mol^{-1} relative to **4** in dichloromethane solution). In solution, this **4**·2MeOH species was then used as a reference for the energies and all results are expressed relative to it and reported as ΔE (kcal mol^{-1}) (Scheme 4).

In contrast with the gas-phase results, the protonation of the metal by the carboxyl group in the **4a** species renders the hydrido intermediate **4b** with an energy of +26.5 kcal mol^{-1} relative to **4a**·2MeOH, which is reached after TS'_{4a-4b} at 27.6 kcal mol^{-1}. As shown above, this hydrido species is a shallow minimum unstable to a gas-phase reoptimization. It is followed by TS'_{4b-1} at 34.6 kcal mol^{-1} and eventually leads to **1**, which is slightly endoergic at this level of calculation (+1.7 kcal mol^{-1}). This transition state is only 1.5 kcal mol^{-1} above TS'_{4c-1} in the methanol-assisted pathway. The methanol-assisted processes are qualitatively similar in the gas phase and in solution, although the energies involved in the latter reflect the large stabilization of **4a**·2MeOH. The hydrido intermediate **4c**·MeOH located at 9.4 kcal mol^{-1} is reached through TS'_{4-4c} with an activation energy of 22.1 kcal mol^{-1} above **4a**·2MeOH. From the hydrido intermediate **4c**·MeOH, after loss of the hydrogen-bonded methanol molecule through TS'_{4c-1} at 33.1 kcal mol^{-1} (slightly lower than TS'_{4b-1}), **1** is reached (see the Supporting Information). As in the gas phase, the solvent-assisted pathway shows the most feasible formation of the key hydrido intermediate, although in fact the limiting step of the reaction is the insertion step in both pathways (Scheme 4).

Interestingly, solvent-mediated proton transfer has been recently reported to be involved in a series of processes such as formation of hydrido intermediates,[18] heterolytic hydrogen splitting,[19] alkyne to vinylidene isomerization,[20] and addition reactions[21] or H/D exchange,[22] among others. The role of solvent as a proton shuttle for proton transfer reactions has also been evidenced in several gold-catalyzed reactions.[23]

Imino and Pyridinediacetic Acid Derivatives As Potential ONO Pincer Ligand Precursors. In order to investigate the key factors behind the synthesis of these unusual unsaturated σ,π-cyclooctenyl iridium(III) complexes, we have studied the potential of other dicarboxylic acids for the preparation of related complexes having different pincer ligands. In particular, we have used the iminodiacetic acid

dx.doi.org/10.1021/om400767d | Organometallics XXXX, XXX, XXX−XXX

derivatives $RN(CH_2COOH)_2$ (R = Me, Ph) as precursors for dianionic tridentate pincer ONO ligands. In contrast to the rigidity of 2,6-pyridinedicarboxylate, the remarkable flexibility of these ligands allows for the accommodation of different coordination environments, and in fact, both *fac*[24] and *mer*[25] dispositions have been found in octahedral transition-metal complexes (R = Me).

The reaction of $[Ir(\mu\text{-OMe})(cod)]_2$ with *N*-methyliminodiacetic acid in THF for 3 h at 50 °C gave an orange solution from which the compound $[Ir\{\kappa^2\text{-MeN}(CH_2COOH)(CH_2COO)\}(cod)]$ (**5**) was isolated as an air-sensitive yellow-orange solid in good yield. Compound **5** is silent under ESI conditions, and satisfactory elemental analyses could not be obtained because of its air sensitivity. However, the mononuclear formulation relies on key features of the NMR spectra. The integrity of the cod ligand in **5** became evident both in the ^1H and $^{13}C\{^1H\}$ NMR spectra (CD_3OD), which showed four well-defined resonances for the =CH protons and carbons, denoting the lack of symmetry in the molecule. Most probably **5** is a neutral iridium(I) species having a monodeprotonated κ^2-*N,O* coordinated *N*-methyliminodiacetic acid and a free carboxymethyl group (Figure 4).[26] The $^1H-^1H$ COSY related resonances at 5.00/4.85 and 4.63/4.32 ppm correspond to the =CH protons of the double bonds *trans* to the N and O atoms, respectively.[27] Signals for the inequivalent $>CH_2$ of the 2-((carboxymethyl)(methyl)amino)acetate ligand were observed at 71.2 and 69.0 ppm in the $^{13}C\{^1H\}$ NMR and as two AB quartets centered at 3.83 and 3.68 ppm ($J_{AB} \approx 16$ Hz) in the ^1H NMR spectra. Interestingly, two protons of each AB system are mutually coupled ($J_{H-H} = 1.8$ Hz), resulting in a set of resonances with an unusual shape (Figure 4). The carboxyl group in **5** was not observed, probably due to H/D exchange with CD_3OD.

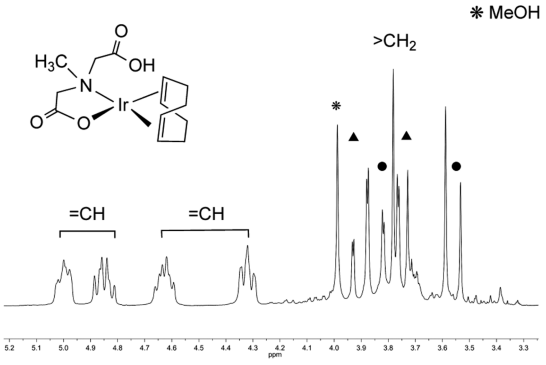

Figure 4. Selected region of the ^1H NMR spectrum of $[Ir\{\kappa^2\text{-MeN}(CH_2COOH)(CH_2COO)\}(cod)]$ (**5**).

Compound **5** is formally an analogue of the intermediate species $[Ir(\kappa^2\text{-Hpydc})(cod)]$ proposed in the formation of **1**. However, the intramolecular proton transfer to the iridium center from the carboxyl group in **5** does not take place and the formation of a related σ,π-cyclooctenyl iridium(III) complex was not observed. A comparison of the acidic strengths of H_2pydc ($pK_{a1} = 2.10$ and $pK_{a2} = 4.38$)[28] and MeN-$(CH_2COOH)_2$ ($pK_{a1} = 2.50$, $pK_{a2} = 9.50$)[29] evidenced the less acidic character of *N*-methyliminodiacetic acid. Despite having very similar first acid dissociation constants, K_{a1}, the second acid dissociation constants, K_{a2}, differ by 5 orders of magnitude. Thus, the acidity of the COOH proton appears to play a key role in the proton transfer process, which is in full agreement with the behavior observed in oxidative addition reactions of carboxylic acids to $[Ir(cod)(PMe_3)_3]Cl$.[14b] Interestingly, the related *N*-phenyliminodiacetic acid PhN-$(CH_2COOH)_2$ has acidic properties very similar to those of H_2pydc ($pK_{a1} = 2.40$, $pK_{a2} = 4.96$),[30] and thus, its reactivity has been investigated.

Addition of a methanol solution of $PhN(CH_2COOH)_2$ to a solution of $[Ir(\mu\text{-OMe})(cod)]_2$ in dichloromethane resulted in the formation of a red solid, compound **6**, irrespective of the stoichiometric ratio (1:1 or 2:1). The infrared spectrum of **6** did not show any broad absorption in the −OH stretching region, which confirms that both carboxyl groups have been deprotonated. Unfortunately, the low solubility of this compound precludes further characterization by NMR. In the same way, reaction of the related cyclooctene iridium hydroxy-

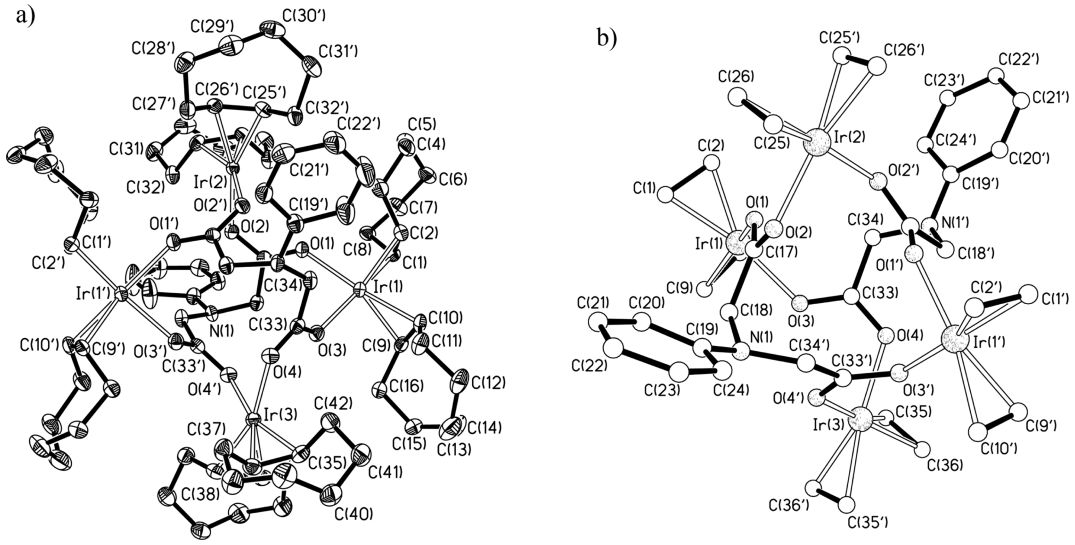

Figure 5. (a) Molecular structure of $[Ir_4\{\kappa^4\text{-PhN}(CH_2COO)_2\}_2(coe)_8]$ (**7**). Primed atoms are related to the unprimed ones by the symmetry transformation $1.5 - x$, $0.5 - y$, z. Hydrogen atoms have been omitted for clarity. (b) Schematic drawing showing the κ^4 coordination of each *N*-phenyliminodicarboxylate group in **7** (only the olefinic carbons of the cyclooctene ligands have been represented).

dx.doi.org/10.1021/om400767d | *Organometallics* XXXX, XXX, XXX−XXX

Table 1. Selected Bond Distances (Å) and Angles (deg) for the Tetranuclear Complex $[Ir_4\{\kappa^4\text{-PhN}(CH_2COO)_2\}_2(coe)_8]$ (7)

Bond Distances			
Ir(1)−O(1)	2.105(2)	Ir(1)−O(3)	2.112(2)
Ir(1)−C(1)	2.109(3)	Ir(1)−C(9)	2.096(3)
Ir(1)−C(2)	2.101(3)	Ir(1)−C(10)	2.122(3)
Ir(2)−O(2)	2.105(2)	Ir(3)−O(4)	2.099(2)
Ir(2)−C(25)	2.106(3)	Ir(3)−C(35)	2.120(3)
Ir(2)−C(26)	2.114(3)	Ir(3)−C(36)	2.100(3)
C(1)−C(2)	1.415(5)	C(9)−C(10)	1.407(5)
C(25)−C(26)	1.412(5)	C(35)−C(36)	1.416(5)
Bond Angles[a]			
O(1)−Ir(1)−O(3)	85.12(9)	O(3)−Ir(1)−M(1)	172.14(9)
O(1)−Ir(1)−M(1)	91.08(9)	O(3)−Ir(1)−M(2)	91.11(9)
O(1)−Ir(1)−M(2)	173.05(9)	M(1)−Ir(1)−M(2)	93.35(10)
O(2)−Ir(2)−O(2′)	84.54(13)	O(4)−Ir(3)−O(4′)	83.59(12)
O(2)−Ir(2)−M(3)	91.52(10)	O(4)−Ir(3)−M(4)	92.11(10)
O(2)−Ir(2)−M(3′)	174.47(10)	O(4)−Ir(3)−M(4′)	174.84(10)
M(3)−Ir(2)−M(3′)	92.67(10)	M(4)−Ir(3)−M(4′)	92.31(10)

[a]M(1), M(2), M(3), and M(4) represent the midpoints of the C(1)−C(2), C(9)−C(10), C(25)−C(26), and C(35)−C(36) olefinic double bonds, respectively. Primed atoms are related to the unprimed atoms by the symmetry transformation 1.5 − x, 0.5 − y, z.

bridged complex $[Ir(\mu\text{-OH})(coe)_2]_2$ with $PhN(CH_2COOH)_2$ under the same conditions gave an insoluble yellow-orange solid that has been characterized as the tetranuclear complex $[Ir_4\{\kappa^4\text{-PhN}(CH_2COO)_2\}_2(coe)_8]$ (**7**) by a single-crystal X-ray diffraction study. The formation of **7** probably results from the fast intermolecular deprotonation of the free −COOH arm by $[Ir(\mu\text{-OH})(coe)_2]_2$ in the likely intermediate $[Ir\{\kappa^2\text{-PhN}(CH_2COOH)(CH_2COO)\}(coe)_2]$. The IR spectra of compounds **6** and **7** are comparable, which allows us to propose a similar tetranuclear formulation for $[Ir_4\{\kappa^4\text{-PhN}(CH_2COO)_2\}_2(cod)_4]$ (**6**) with a closely related structure derived from the replacement of coe ligands by cod. **6** and **7** were obtained in 80% and 90% yields, respectively, using the correct stoichiometric ratio. Crystals of **7** suitable for X-ray analysis were obtained by slow diffusion of solutions of both reactants in the corresponding solvents. The molecular structure of **7** is shown in Figure 5, and Table 1 collects the most relevant bond parameters.

The complex is tetranuclear, but only half of the molecule is crystallographically independent. The molecule exhibits C_2 symmetry with an intramolecular crystallographic 2-fold axis passing through the Ir(2) and Ir(3) atoms. According to this, the four metal atoms conform a strictly planar, almost perfect square, with the metal atoms separated well over 5 Å and with each iridium atom bonded to the olefinic bonds of two cyclooctene ligands. Each tetradentate iminodicarboxylate ligand is linked to all four metals, with each pair of oxygens of each carboxylate group bridging two contiguous metals, in an alternate way at both sides of the metal square, having an uncoordinated amine group (Figure 5b). All four metals exhibit slightly distorted square-planar environments typical of Ir(I) atoms; it is noteworthy to point out that while the Ir(1) coordination plane is almost coplanar with the tetrametallic square skeleton (dihedral angle 13.26(5)°), those of Ir(2) and Ir(3) are nearly perpendicular (mean 83.57(5)°) to the tetrametallic reference plane.

The metal coordination bond distances, Ir−C and Ir−O, show very similar values, with all of the figures within very narrow ranges, 2.096−2.122(3) and 2.099−2.112(2) Å, respectively, which substantiates the identical electronic nature of all four metals. The Ir−O bond lengths are very similar to those reported in other related carboxylate-bridged dinuclear Ir(I) complexes such as $[Ir(\mu\text{-}O_2C_8H_{15})(cod)]_2$ ($O_2C_8H_{15}$ = 2-ethylhexanoate), with a mean value of 2.097(3) Å,[31] or in the polymeric $[IrAg(\mu\text{-}O_2CCF_3)_2(cod)]_n$, where the "Ir($\mu$-O-carboxylate)$_2$(olefin)$_2$" units are also present (mean 2.095(5) Å).[32] The average olefinic C═C bond length, 1.413(3) Å, compares well with other bis-cyclooctene κ^2-O,O iridium complexes[33] (mean 1.417(8) Å); this value is clearly longer than the free olefinic C═C double bond (mean 1.316(15) Å)[34] and should be interpreted as the result of the electron-rich Ir(I) engaging in a high degree of π back-bonding.

The results described above strongly suggest that the acidity of the dicarboxylic compound is not the only factor that controls the formation of the unsaturated σ,π-cyclooctenyl iridium(III) complexes. In spite of its weaker Brønsted basicity, the stronger N-coordination ability of the pyridine fragment versus that of the aliphatic amines also should play an important role in the protonation step. In order to test this hypothesis, the reactivity of 2,2′-(pyridine-2,6-diyl)diacetic acid, $py(CH_2COOH)_2$ (pK_{a1} = 3.08, pK_{a2} = 5.92), was studied.[28] The reaction with standard dinuclear and mononuclear iridium starting materials invariably led to the formation of scarcely soluble yellow solids with poorly resolved NMR spectra without any evidence for the formation of a σ,π-cyclooctenyl iridium(III) complex. Thus, both the acidity and the rigidity of the tridentate ligand are determinant factors in the formation of $\sigma-\pi$-cyclooctenyl iridium(III) complexes. As it has been shown before, the key transition state for the proton transfer requires a rigid structure in order to allow the carboxylic group to approach the iridium center. However, in the case of highly flexible tridentate ligands the freedom of the carboxyl group and its fast intermolecular deprotonation by iridium dinuclear complexes probably determines the course of the reaction.

Reactivity of $[Ir(\kappa^3\text{-pydc})(1\text{-}\kappa\text{-}4,5\text{-}\eta\text{-}C_8H_{13})]$ with Monodentate N- and P-Donor Ligands. Although iridium(III) complexes are usually inert to substitution, the presence of strong labilizing ligands can promote ligand replacement reactions. The *trans* influence exerted by the iridium−alkyl bond in the solvate $[Ir(\kappa^3\text{-pydc})(1\text{-}\kappa\text{-}4,5\text{-}\eta\text{-}C_8H_{13})(MeOH)]$ (**1**·MeOH) points to a labile methanol ligand. Thus, complex **1** can be considered an unsaturated iridium(III) complex and,

dx.doi.org/10.1021/om400767d | *Organometallics* XXXX, XXX, XXX−XXX

consequently, methanol replacement by more coordinating N- and P-donor ligands could be possible.

Reaction of **1** with an excess of pyridine or benzylamine gave the corresponding complexes [Ir(κ^3-pydc)(1-κ-4,5-η-C_8H_{13})(py)] (**1-py**) and [Ir(κ^3-pydc)(1-κ-4,5-η-C_8H_{13})($BnNH_2$)] (**1-$BnNH_2$**), which were isolated as yellow solids in excellent yields (Scheme 5). Under similar conditions, 2-picoline did not react with **1**, probably due to steric constraints. The complexes **1-py** and **1-$BnNH_2$** were fully characterized by spectroscopic means and elemental analysis. The coordination of the N-donor ligands is confirmed in the ^{1}H NMR spectra, where the expected set of resonances for the σ,π-cyclooctenyl ligand was also observed. A characteristic sign for the ligand exchange reaction is the downfield shift by 2−3 ppm of the Ir−CH− resonance (C-1) in the $^{13}C\{^1H\}$ NMR spectra upon the coordination of the N-donor ligands in *trans* positions.

Scheme 5. Mononuclear Complexes Derived from 1

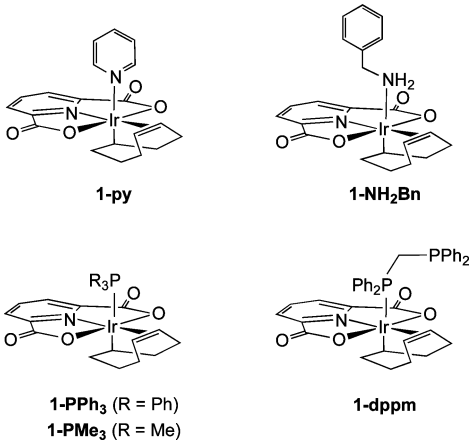

The molecular structure of **1-py** has been determined by an X-ray analysis, and it is shown in Figure 6. The iridium center exhibits a distorted-octahedral environment with links to the tridentate meridional O,N,O-coordinated pyridinedicarboxylate, to the formally bidentate σ,π-cyclooctenyl ligand, and to the nitrogen of the pyridine group. The iridium configuration is such that the olefinic bond is situated *trans* to the nitrogen of the pydc ligand, while the alkylic cyclooctenyl carbon is also positioned *trans* to the pyridine group. Major distortions from the octahedral coordination arise from the chelating units within the tridentate pydc group (mean N−Ir−O = 78.83(9)°) and, in a minor extension, from the chelating nature of the σ,π-bonded cyclooctenyl ligand (C(11)−Ir−M = 84.64(15)°). The pydc ligand is strictly planar and defines a meridional metal coordination plane where the olefin exhibits an in-plane conformation (line-plane angle 1.5(3°)).

The most relevant structural feature of this molecule is the long Ir−N(2) bond length, 2.209(3) Å, a clear consequence of the high structural *trans* effect of the Ir−alkyl bond. Similar Ir−N bond distances have been observed in Ir(III) complexes where the pyridine molecule is coordinated to the iridium *trans* to a high *trans*-influence ligand: this is the case in [Ir(acac)$_2$R(py)], where R is the cyclohexyl group (Ir−N = 2.225(6) Å, Ir−C = 2.060(7) Å)[7c] or a vinyl moiety (Ir−N = 2.209(14) Å, Ir−C = 1.97(3) Å),[35] and also when the pyridine group occupies a position *trans* to a hydride ligand ([Ir(PCy_3)(Py)$_3$H$_2$]$^+$; Ir−N = 2.216(2) and 2.2101(19) Å)[36] or to a metal−metal bond such as in [Ir(μ-O_2CCH_3)(CO)Cl(py)]$_2$ (Ir−N = 2.200(5) Å).[37]

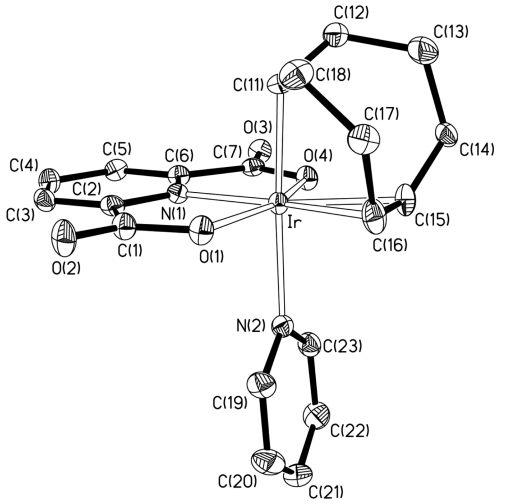

Figure 6. Molecular structure of [Ir(κ^3-pydc)(1-κ-4,5-η-C_8H_{13})(py)] (**1-py**). Bond distances (Å) and angles (deg): Ir−O(1) = 2.078(3), Ir−O(4) = 2.076(3), Ir−N(1) = 1.981(3), Ir−N(2) = 2.209(3), Ir−C(11) = 2.079(4), Ir−C(15) = 2.175(4), Ir−C(16) = 2.178(4), C(15)−C(16) = 1.373(6); O(1)−Ir−O(4) = 157.62(11), O(1)−Ir−N(1) = 78.80(12), O(4)−Ir−N(1) = 78.86(12), N(1)−Ir−M = 177.02(12), N(2)−Ir−C(11) = 176.30(15), C(11)−Ir−M = 84.64(15). M represents the midpoint of the olefinic C(15)−C(16) double bond.

Although no iridium structure has been reported including the pincer tridentate pydc ligand, a vast piece of Ir(III) structural chemistry has been described with different substituted derivatives for the N,O-bidentate pyridine-2-carboxylate group.[38] It is remarkable that in all these complexes the Ir−N interaction (2.014−2.215 Å) is surprisingly longer than the distance observed in **1-py** (1.981(3) Å). Additionally, the Ir−O bonds in **1-py** seem also to be stronger (2.078 and 2.076(3) Å) than the usual Ir−O interaction in the bidentate pyridinecarboxylate complexes (range 2.033−2.194 Å).[38] Both facts are solid-state evidence of the reported special stabilization associated with the pincer ligands, particularly for pydc.[11] As a consequence of the noted strong Ir−pydc interaction and also of the higher oxidation state of the metal atom in **1-py** (in comparison to that observed in **6**), the Ir−olefin bond seems to be very weak, as evidenced by the relatively long Ir−C bond lengths (2.175 and 2.178(4) Å) and by the short C═C distance of 1.373(6) Å (weak π-back-donation), only slightly elongated from the ideal value of a free double bond (1.316(15) Å).[34]

Compounds [Ir(κ^3-pydc)(1-κ-4,5-η-C_8H_{13})(PPh_3)] (**1-PPh_3**) and [Ir(κ^3-pydc)(1-κ-4,5-η-C_8H_{13})(PMe_3)] (**1-PMe_3**) (Scheme 4) were prepared by reacting **1** with 1 equiv of the corresponding phosphine ligand and isolated as lemon yellow solids in excellent yields. The $^{31}P\{^1H\}$ NMR of the complexes showed the expected singlet resonances at −7.23 (**1-PPh_3**) and −38.98 ppm (**1-PMe_3**). In addition, the coordination of the PR_3 ligands *trans* to the iridium−alkyl bond of the cyclooctenyl ligand is supported by the large J_{C-P} coupling of the Ir−CH− resonance (C-1) in the $^{13}C\{^1H\}$ NMR spectra, which was observed at 31.72 (J_{C-P} = 85.8 Hz) and 31.29 ppm (J_{C-P} = 91.5 Hz), respectively. It is noticeable that an excess of PR_3 does not induce the decoordination of either the σ,π-cyclooctenyl or the

dx.doi.org/10.1021/om400767d | *Organometallics* XXXX, XXX, XXX−XXX

pincer ligands, which demonstrates the outstanding stability of the rigid molecular framework in **1**.

Reactivity of [Ir(κ^3-pydc)(1-κ-4,5-η-C_8H_{13})] with Bidentate P-Donor Ligands. In order to induce a possible change in the coordination mode of the σ,π-cyclooctenyl moiety in [Ir(κ^3-pydc)(1-κ-4,5-η-C_8H_{13})] (**1**), we have explored its reactivity with chelating diphosphines. Reaction of **1** with 1 equiv of bis(diphenylphosphino)methane (dppm) gave [Ir(κ^3-pydc)(1-κ-4,5-η-C_8H_{13})(κ^1-dppm)] (**1-dppm**), which features a monocoordinated dppm ligand (Scheme 5). The compound, which was obtained as a lemon yellow solid in 87% yield, has been fully characterized in solution by spectroscopic methods and in the solid state by a single-crystal X-ray analysis. The presence of a κ^1-dppm coordinated ligand became evident in the $^{31}P\{^1H\}$ NMR spectrum, which showed two strongly coupled doublet resonances at −17.47 and −27.81 ppm (J_{P-P} = 70.7 Hz) corresponding to the coordinated and uncoordinated P donor atoms, respectively.[39] On the other hand, the coordination of the dppm ligand *trans* to the Ir−CH− bond of the σ,π-cyclooctenyl ligand was derived from the large J_{C-P} coupling of 86.2 Hz observed for the C-1 resonance at 31.57 ppm in the $^{13}C\{^1H\}$ NMR spectrum. In addition, the >CH_2 resonance of the dppm ligand was observed as a doublet of doublets at 23.96 ppm with J_{C-P} couplings of 31.2 and 16.7 Hz.

The molecular structure of **1-dppm** is shown in Figure 7. This molecule resembles quite well that of **1-py**, in which the pyridine group has been substituted by a monodentate P-bonded dppm ligand. The complex exhibits an analogous octahedral coordination, with the same stereodistribution of ligands and statistically identical molecular parameters for the pydc and for the σ,π-bonded cyclooctenyl ligands. Only the Ir−C bond distances of the coordinated olefinic group are significantly longer (mean 2.215(6) Å in **1-dppm**) than those observed in **1-py** (2.176(3) Å), although the C=C bond distance does not vary accordingly (1.387(13) vs 1.373(6) Å).

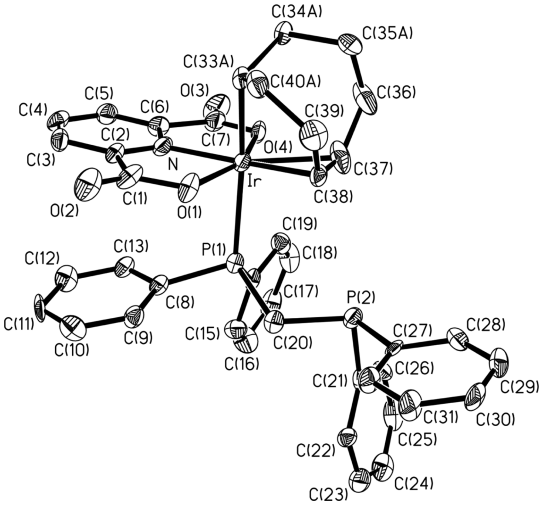

Figure 7. Molecular structure of [Ir(κ^3-pydc)(1-κ-4,5-η-C_8H_{13})(κ^1-dppm)] (**1-dppm**). Bond distances (Å) and angles (deg): Ir−O(1) = 2.074(6), Ir−O(4) = 2.057(6), Ir−N(1) = 1.975(6), Ir−P(1) = 2.458(2), Ir−C(33A) = 2.108(14), Ir−C(37) = 2.225(9), Ir−C(38) = 2.204(8), C(37)−C(38) = 1.387(13); O(1)−Ir−O(4) = 157.1(2), O(1)−Ir−N(1) = 78.3(3), O(4)−Ir−N(1) = 78.8(3), N(1)−Ir−M = 171.3(3), P(1)−Ir−C(33A) = 167.6(5), C(33A)−Ir−M 81.7(5). M represents the midpoint of the olefinic C(37)−C(38) double bond; bond parameters involving C(33) are only expressed for the disordered carbon atom of higher occupancy.

A remarkable difference of this molecule in comparison with **1-py** is the deviation of the olefinic carbons from the strictly planar meridional plane described by the three donor atoms of the pyridinedicarboxylate group and the metal atom; while in **1-py** the olefin fits reasonably in this plane (N−Ir−M = 177.02(12)°), in **1-dppm** the olefin is clearly out of this plane by a mean value of 0.322(8) Å, with a closer N−Ir−M bond angle of 171.3(3)°. Most probably this fact should be associated with the bulkier character of dppm in comparison to pyridine.

As noted for the pyridine in **1-py**, the high structural *trans* effect of the alkylic Ir−C bond elongates the Ir−P(1) bond length to a value of 2.458(2) Å. As far as we know, this is the longest Ir−P bond distance observed in a Ir(III) complex containing a PR_3 phosphine situated *trans* (C−Ir−P > 160°) to an alkylic sp^3 carbon (range 2.276−2.410 Å, mean 2.343(2) Å).[37] If the metal complex should contain a dppm ligand, the longest Ir−P separation (*trans* to an alkylic carbon) described so far is 2.382(1) Å in [$IrMe_2$(dppm)$_2$][OTf].[40] All these facts evidence a weak bonding interaction between the metal and the monodentate diphosphine.

Reaction of **1** with 1 equiv of 1,2-bis(diphenylphosphino)-ethane (dppe) gave a yellow solid that consists of roughly a 1/1 mixture of [Ir(κ^3-pydc)(1-κ-4,5-η-C_8H_{13})(κ^1-dppe)] (**1-dppe**) and the dinuclear compound [Ir(κ^3-pydc)(1-κ-4,5-η-C_8H_{13})]$_2$(μ-dppe) (**1$_2$-dppe**), having a dppe ligand bridging two [Ir(κ^3-pydc)(1-κ-4,5-η-C_8H_{13})] fragments (Scheme 6).

Scheme 6. Dinuclear Complexes Derived from 1

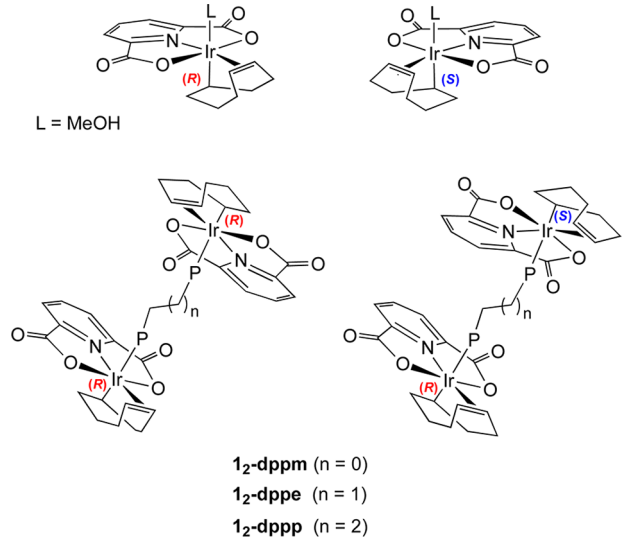

The $^{31}P\{^1H\}$ NMR (121.49 MHz) spectrum of this mixture in CD_2Cl_2 at room temperature showed a set of three broad resonances, suggesting a fluxional behavior. However, the spectrum at 223 K featured well-defined resonances. The two coupled resonances at −12.12 and −14.17 ppm (J_{P-P} = 32 Hz) were assigned to **1-dppe** and the two signals at −10.89 and −11.09 ppm to the two diastereoisomers of **1$_2$-dppe** (see below). Most probably, both species are in a dppe-mediated dynamic equilibrium[41] that causes resonances to broaden at room temperature:

2 **1-dppe** ⇄ **1$_2$-dppe** + dppe

dx.doi.org/10.1021/om400767d | *Organometallics* XXXX, XXX, XXX−XXX

The dinuclear complex **1_2-dppm** has been isolated from the solution obtained after dissolving a solid mixture of **1** and 1/2 equiv of dppm in CH_2Cl_2/MeOH (3/1). This method has also revealed to be useful for the synthesis of the compounds **1_2-dppe** and **1_2-dppp** using the corresponding diphosphines. The complexes have been obtained as yellow solids in yields of over 80% and fully characterized by elemental analysis, mass spectra, and multinuclear NMR spectroscopy. The ESI spectra of the three compounds showed the molecular ions of the mononuclear complexes [**1-diphos**]$^+$ resulting from the loss of one of the iridium fragments. However, the ESI spectrum of **1_2-dppe** showed the molecular ion at m/z 1329.2 with the right isotopic distribution.

The C-1 atom of the $\sigma-\pi$ cyclooctenyl ligand in **1** is a stereogenic center, and thus, compound **1** is chiral and exists as a pair of enantiomers, namely (R_C)-**1** and (S_C)-**1**. The assembly of the dinuclear compounds **1_2-(μ-diphos)** can produce three stereoisomers: the enantiomeric pair [(R_C)-**1**]$_2$(μ-diphos)/[(S_C)-**1**]$_2$(μ-diphos) (indistinguishable by NMR) and [(R_C)-**1**][(S_C)-**1**](μ-diphos), with C_2 and C_s symmetries, respectively (Scheme 5). As expected, the dinuclear compounds exist as a 1/1 mixture of both diastereoisomers, which have been observed in the $^{31}P\{^1H\}$ NMR spectra as two single resonances (see the Experimental Section). In addition, the C-1 resonances of the equivalent σ,π-cyclooctenyl ligands in both diastereoisomers of **1_2-dppe** were observed as doublets of doublets at 32.55 and 32.41 ppm in the $^{13}C\{^1H\}$ NMR spectrum with J_{C-P} coupling constants of 90.0 and 2.2 Hz, which further supports the proposed structure.

CONCLUSIONS

The synthesis of the unusual σ,π-cyclooctenyl iridium(III) pincer compounds [Ir(κ^3-pydc-X)(1-κ-4,5-η-C_8H_{13})] can be accomplished by several routes, involving the corresponding 4-substituted 2,6-pyridinedicarboxylic acids or their lithium salts and standard mono- or dinuclear iridium complexes. An investigation of the mechanism of the reaction has shown the initial formation of the species [Ir(κ^2-Hpydc)(cod)] having a κ^2-N,O coordinated monodeprotonated ligand. Deuterium labeling studies in combination with theoretical calculations at the DFT level have shown that the formation of the σ,π-cyclooctenyl iridium(III) complexes involves a metal-mediated proton transfer to the 1,5-cyclooctadiene ligand through the methanol-stabilized hydrido species [IrH(κ^2-pydc)(cod)-(CH_3OH)]. Remarkably, the formation of this key hydrido intermediate results from the solvent-assisted proton transfer through a hydrogen-bonding network involving a carboxyl group, a methanol molecule, and the iridium center, forming an eight-membered metallacycle.

The application of this synthetic methodology with related dicarboxylic acid precursors to dianionic tridentate pincer ONO complexes has shown a narrow scope. However, the reactivity of some iminodiacetic acid derivatives, RN(CH_2COOH)$_2$ (R = Me, Ph), has allowed us to identify the acidity (pK_a) and the rigidity of the potential tridentate ligand precursor as the key factors leading to σ,π-cyclooctenyl iridium(III) complexes.

[Ir(κ^3-pydc)(1-κ-4,5-η-C_8H_{13})] behaves as an unsaturated species, and coordination of some monodentate N- and P-donor ligands has led to the preparation of octahedral complexes. The stability of the rigid molecular framework has allowed for the preparation of diphosphine-bridged dinuclear assemblies that have been obtained as a mixture of two diastereoisomers. Interestingly, in the case of the short-bite bis(diphenylphosphino)methane ligand the nuclearity can be modulated and a mononuclear complex having a κ^1-dppm ligand has been also prepared.

EXPERIMENTAL SECTION

General Considerations. All experiments were carried out under an atmosphere of argon using Schlenk techniques or a glovebox. Solvents were obtained from a Solvent Purification System (Innovative Technologies). CD_2Cl_2 and DMSO-d_6 (Euriso-top) were dried using activated molecular sieves. Methanol-d_4 (<0.02% D_2O, Euriso-top) was used as received. Elemental analyses were carried out with a PerkinElmer 2400 CHNS/O analyzer. NMR spectra were recorded on Bruker AV-400 and AV-300 spectrometers. Chemical shifts are reported in ppm relative to tetramethylsilane and referenced to partially deuterated solvent resonances. Coupling constants (J) are given in hertz. Spectral assignments were achieved by a combination of $^1H-^1H$ COSY, ^{13}C DEPT, APT, $^1H-^{13}C$ HSQC, and $^1H-^{13}C$ HMBC experiments. The numbering scheme used in the NMR data of the compounds is shown in Figure 1. Electrospray mass spectra (ESI-MS) were recorded on a Bruker MicroTof-Q instrument using sodium formate as reference. MALDI-TOF mass spectra were obtained on a Bruker Microflex mass spectrometer using DCTB (*trans*-2-[3-(4-*tert*-butylphenyl)-2-methyl-2-propenylidene]malononitrile) or dithranol as the matrix. Standard literature procedures were used to prepare the starting materials [Ir(μ-OMe)(cod)]$_2$,[42] [Ir(μ-OH)(coe)$_2$]$_2$,[43] and [Ir(cod)($NCCH_3$)$_2$]PF_6.[44] Pyridine-2,6-dicarboxylic acid (H_2pydc) and *N*-methyliminodiacetic and *N*-phenyliminodiacetic acids were obtained from Fluka, Aldrich, and Acros, respectively, and used as received. 4-Bromopyridine-2,6-dicarboxylic acid (Hpydc-Br) was prepared from chelidamic acid (4-hydroxypyridine-2,6-dicarboxylic acid, Fluka) following the procedure described in the literature.[45]

Lithium Pyridine-2,6-dicarboxylate (Li_2pydc). To a suspension of 2,6-pyridinedicarboxylic acid (0.268 g, 1.60 mmol) in diethyl ether (20 mL) was added dropwise a 1.6 M solution of *n*-BuLi in hexane (2.0 mL, 3.2 mmol) with stirring at 195 K. The reaction mixture was warmed to room temperature within 1 h. During this time, the suspension turned from white to pale yellow. The resulting suspension was concentrated, decanted, and filtered to afford an off-white solid, which was washed with diethyl ether (3 × 10 mL) and dried in vacuo. Yield: 0.279 g (97%). ^1H NMR (400.16 MHz, 298 K, DMSO-d_6): δ 8.24 (m, 2H), 8.18 (m, 1H).

Lithium 6-Carboxypicolinate (HLipydc). 2,6-Pyridinedicarboxylic acid (0.268 g, 1.60 mmol) and *n*-BuLi in hexane (1.0 mL, 1.6 mmol) were reacted in diethyl ether (20 mL) at 195 K. Workup as described above gave the salt as an off-white solid. Yield: 0.263 g (95%). ^1H NMR (400.16 MHz, 298 K, DMSO-d_6): δ 13.38 (br, 1H, −COOH), 8.23 (m, 2H), 8.17 (m, 1H).

[Ir(κ^3-pydc)(1-κ-4,5-η-C_8H_{13})] (1). *Method A.* [Ir(μ-OMe)(cod)]$_2$ (0.132 g, 0.200 mmol) and H_2pydc (0.068 g, 0.40 mmol) were reacted in a CH_2Cl_2/MeOH mixture (3/1, 20 mL) for 14 h to give a bright yellow solution. The solution was brought to dryness in vacuo and the crude compound dissolved in a CH_2Cl_2/MeOH (20/1) mixture (2 mL) and then eluted through an alumina column (5 × 1.5 cm) to give a yellow solution. Concentration of the solution to ca. 1 mL and slow addition of diethyl ether gave the compound as a yellow solid, which was filtered, washed with diethyl ether (2 × 3 mL), and dried in vacuo. Yield: 0.170 g (85%).

Method B. A solid mixture of [Ir(cod)(CH_3CN)$_2$]PF_6 (0.106 g, 0.200 mmol) and LiHpydc (0.035 g, 0.200 mmol) was dissolved in a CH_2Cl_2/MeOH mixture (3/1, 20 mL). The resulting red solution was stirred for 14 h to give a bright yellow solution. The solution was filtered and then concentrated under vacuum to ca. 5 mL. Slow addition of diethyl ether (20 mL) gave the compound as a yellow solid that was filtered, washed with diethyl ether, and dried under vacuum. Yield: 0.096 g (96%).

Method C. [Ir(cod)(CH_3CN)$_2$]PF_6 (0.106 g, 0.200 mmol) and Li_2pydc (0.036 g, 0.200 mmol) were reacted in a CH_2Cl_2/MeOH mixture (3/1, 20 mL) for 14 h to give a bright yellow solution. Workup as described above (method B) afforded the compound as a

dx.doi.org/10.1021/om400767d | *Organometallics* XXXX, XXX, XXX−XXX

yellow solid. Yield: 0.090 g (90%). The analytical and spectroscopic data evidenced that compound **1** was actually isolated as the methanol solvate **1**·MeOH.[11] Anal. Found: C, 38.42; H, 3.98; N, 2.75. Calcd for $C_{15}H_{16}IrNO_4.CH_3OH$: C, 38.54; H, 4.04; N, 2.81 (method B).

[Ir(κ^3-pydc)(1-κ-4,5-η-$C_8H_{12}D$)] (1-d_1). A solid mixture of [Ir(cod)(CH_3CN)$_2$]PF_6 (0.053 g, 0.10 mmol) and [Li_2pydc] (0.018 g, 0.10 mmol) was dissolved in $CD_2Cl_2/CD_3OD/D_2O$ (4.2 mL, 3/1/0.1, respectively). The solution stirred at room temperature for 14 h and then directly analyzed by NMR. ^{1}H NMR (400.16 MHz, 298 K, CD_2Cl_2/CD_3OD): δ 8.35 (t, J_{H-H} = 7.8 Hz, 1H, 4-H), 8.18 (dd, J_{H-H} = 7.8 and 1.2 Hz, 1H, 3-H or 5-H), 8.12 (dd, J_{H-H} = 7.8 and 1.2 Hz, 1H, 3-H or 5-H) (pydc), 5.81 (dt, J_{H-H} = 9.1 and 3.0 Hz, 1H, 4-H), 5.59 (d, J_{H-H} = 9.9 Hz, 1H, 5-H), 3.13 (d, J_{H-H} = 15.9 Hz, 1H, 6-H), 2.35 (m, J_{H-H} = 11.0 and 4.3 Hz, 1H, 3-H), 2.29−2.13 (bm, 2H, 3-H and 6-H), 2.01−1.82 (bm, 3H, 1-H, 2-H and 7-H), 1.59 (bd, J_{H-H} = 14.1 Hz, 1H, 7-H), 0.39 (dd, J_{H-H} = 12.3 and 3.6 Hz, 1H, 2-H), 0.01 ppm (d, J_{H-H} = 3.3 Hz, 1H, 8-H) ($C_8H_{12}D$). ^{13}C{^{1}H} NMR (75.48 MHz, 298 K, CD_2Cl_2/CD_3OD): δ 175.55, 175.22 (*C*O), 148.31, 147.17 (C-2 and C-6), 141.30 (C4) (pydc), 89.53 (C-4), 85.08 (C-5), 40.69 (C-2), 34.73 (t, J_{C-D} = 19.0 Hz, C-8), 27.83 (C-6), 26.29 (C-3), 25.07 (C-7), 15.09 (C-1) (1-κ-4,5-η-$C_8H_{12}D$). ^{2}H NMR (61.42 MHz, 298 K, CH_2Cl_2/MeOH): δ 1.21 (s, 1D, $C_8H_{12}D$). MS (MALDI-TOF, DCTB, CH_2Cl_2/MeOH): *m*/*z* 467.9 (M^+), 316.4 (M^+ − pydc).

[Ir(κ^3-pydc-Br)(1-κ-4,5-η-C_8H_{13})] (3). H_2pydc-Br (0.246 g, 1.00 mmol) and [Ir(μ-OMe)(cod)]$_2$ (0.331 g, 0.500 mmol) were reacted in CH_2Cl_2/MeOH (40 mL, 5:1) for 14 h at room temperature to give a red solution. Work up as described above for **1** (method A) gave the compound as red solid. Yield: 0.532 g (94%). Anal. Found: C, 32.05; H, 2.92; N, 2.53. Calcd for $C_{15}H_{15}BrIrNO_4.H_2O$: C, 31.98; H, 3.04; N, 2.49. ^{1}H NMR (400.16 MHz, 298 K, CD_2Cl_2/CD_3OD): δ 8.28 (s, 1H), 8.24 (s, 1H) (3-H and 5-H, pydc-Br), 5.87 (td, J_{H-H} = 8.8 and 3.7 Hz, 1H, 4-H), 5.64 (br, 1H, 5-H), 3.17 (d, J_{H-H} = 15.9 Hz, 1H, 6-H), 2.40−2.10 (m, 3H, 3-H and 6-H), 2.01 (m, 1H, 1-H), 1.97 (d, J_{H-H} = 9.4 Hz, 1H, 2-H), 1.85 (dt, J_{H-H} = 14.1 and 4.6 Hz, 1H, 7-H), 1.63 (t, J_{H-H} = 6.08 Hz, 1H, 7-H), 0.94 (tt, J_{H-H} = 14.6 and 2.4 Hz, 1H, 8-H), 0.40 (dd, J_{H-H} = 14.2 and 9.22, 1H, 2-H), 0.03 (dm, J_{H-H} = 13.8 Hz, 1H, 8-H) (C_8H_{13}). ^{13}C{^{1}H} NMR (75.48 MHz; 298 K; CD_2Cl_2/CD_3OD): δ 172.8 (CO), 147.7, 146.6 (C-2 and C-6), 133.1, 132.8 (C-3 and C-5), 135.6 (C-4) (pydc-Br), 89.0 (C-4), 85.0 (C-5), 39.6 (C-2), 34.1 (C-8), 26.8 (C-6), 25.3 (C-3), 24.0 (C-7), 14.6 (C-1) (C_8H_{13}). MS (MALDI-TOF, DCTB, CH_2Cl_2): *m*/*z* 527.2 (M^+).

[Ir{κ^2-MeN(CH_2COOH)(CH_2COO)}(cod)] (5). A solid mixture of [Ir(μ-OMe)(cod)]$_2$ (0.041 g, 0.062 mmol) and *N*-methyliminodiacetic acid (0.018 g, 0.124 mmol) was dissolved in THF (15 mL) and the solution stirred for 3 h at 50 °C. The solvent was removed under vacuum, and the orange residue was washed with hexane (2 × 2 mL) and then dried in vacuo. Yield: 0.047 g (85%). ^{1}H NMR (400.16 MHz, CD_2Cl_2/CD_3OD, 298 K): δ 5.00 (m, 1H), 4.85 (m, 1H), 4.63 (m, 1H), 4.32 (m, 1H) (=CH, cod), 3.83 (AB q, 2H, δ_A 3.90, δ_B 3.76, J_{AB} = 16.1 Hz, J_{AC} = 1.8 Hz, >CH_2), 3.68 (CD q, 2H, δ_C 3.79, δ_D 3.56, J_{CD} = 16.6 Hz, J_{AC} = 1.8 Hz, >CH_2), 2.89 (s, 3H, −CH_3), 2.80−2.67 (m, 2H), 2.64−2.55 (m, 2H), 2.46 (m, 1H), 2.23 (m, 1H), 1.91 (m, 1H), 1.56 (m, 1H) (>CH_2, cod). ^{13}C{^{1}H} NMR (75.48 MHz, CD_2Cl_2/CD_3OD, 298 K): δ 181.3, 180.4 (*C*O), 87.1, 82.9, 77.7, 76.4 (=CH, cod), 71.2 (>CH_2), 69.0 (>CH_2), 56.4 (−CH_3), 34.7, 31.5, 30.2, 26.1 (>CH_2, cod).

[Ir_4{κ^4-PhN(CH_2COO)$_2$}$_2$(cod)$_4$] (6). A solution of *N*-phenyliminodiacetic acid (0.035 g, 0.167 mmol) in methanol (3 mL) was added to a solution of [Ir(μ-OMe)(cod)]$_2$ (0.111 g, 0.167 mmol) in dichloromethane (3 mL) to give a red solid in 1 min. The solution was decanted, and the solid was washed with methanol (2 × 3 mL) and dried under vacuum. Yield: 0.108 g (80%). Anal. Found: C, 38.46; H, 4.10; N, 1.76. Calcd for $C_{52}H_{66}Ir_4N_2O_8$: C, 38.65; H, 4.12; N, 1.73.

[Ir_4{κ^4-PhN(CH_2COO)$_2$}$_2$(coe)$_8$] (7). A solution of *N*-phenyliminodiacetic acid (0.014 g, 0.068 mmol) in methanol (2 mL) was added to a solution of [Ir(μ-OH)(coe)$_2$]$_2$ (0.058 g, 0.068 mmol) in dichloromethane (2 mL). After 1 min a yellow-orange solid precipitated from the solution. The solution was decanted, and the solid was washed with methanol (2 × 3 mL) and dried under vacuum. Yield: 0.066 g (90%). Anal. Found: C, 48.86; H, 6.35; N, 1.35. Calcd for $C_{84}H_{130}Ir_4N_2O_8$·2CH_3OH: C, 48.51; H, 6.53; N, 1.32. Crystals suitable for X-ray diffraction were obtained by layering a solution of [Ir(μ-OH)(coe)$_2$]$_2$ in dichloromethane over a solution of *N*-phenyliminodiacetic acid in methanol at room temperature.

[Ir(κ^3-pydc)(1-κ-4,5-η-C_8H_{13})(py)] (1-py). The compound was prepared by refluxing a solution of [Ir(κ^3-pydc)(1-κ-4,5-η-C_8H_{13})] (**1**) in neat pyridine and isolated as a yellow solid in 85% yield.[11] Good quality microcrystals for X-ray diffraction were grown by slow diffusion of diethyl ether into a dichloromethane solution of **1-py** at 258 K.

[Ir(κ^3-pydc)(1-κ-4,5-η-C_8H_{13})($BnNH_2$)] (1-$BnNH_2$). Benzylamine (2 mL) was added to a suspension of [Ir(κ^3-pydc)(1-κ-4,5-η-C_8H_{13})] (**1**·MeOH; 0.100 g, 0.200 mmol) in CH_2Cl_2 (20 mL). The reaction mixture was heated at 90 °C for 3 h with stirring to give a yellow solution. The solution was cooled to room temperature and evaporated to dryness in vacuo. Crystallization from CH_2Cl_2/Et_2O at low temperature afforded the compound as lemon yellow microcrystals. Yield: 0.100 g (87%). Anal. Found: C, 46.23; H, 4.54; N, 4.95. Calcd for $C_{22}H_{25}IrN_2O_4$: C, 46.06; H, 4.39; N, 4.88. ^{1}H NMR (400.16 MHz, 298 K, CD_2Cl_2): δ 8.08 (t, 1H, J_{H-H} = 8.0 Hz, 4-H), 7.96 (dd, 1H, J_{H-H} = 7.3 and 1.6 Hz), 7.88 (dd, 1H, J_{H-H} = 7.3 and 1.6 Hz) (3-H and 5-H) (pydc), 7.32−7.22 (m, 4H, −NH_2 and Bn), 7.06 (m, 2H, Bn), 6.93 (m, 1H, Bn) ($BnNH_2$), 5.76 (td, 1H, J_{H-H} = 9.5 and 3.6 Hz, 4-H), 5.41 (d, 1H, J_{H-H} = 8.0 Hz, 5-H) (C_8H_{13}), 3.18 (m, 2H, >CH_2, Bn), 3.02 (d, 1H, J_{H-H} = 16.1 Hz), 2.35 (m, 1H), 2.14−2.03 (m, 2H), 1.88−1.73 (m, 2H), 1.50 (d, 1H, J_{H-H} = 13.2 Hz), 1.37 (m, 1H), 0.89 (t, 1H, J_{H-H} = 13.9 Hz), 0.60 (dd, 1H, J_{H-H} = 13.2 and 9.2 Hz), 0.27 (m, 1H) (C_8H_{13}). ^{13}C{^{1}H} NMR (100.62 MHz, 298 K, CD_2Cl_2): δ 176.36, 176.06 (*C*O), 148.48, 147.46 (C-2 and C-6) (pydc), 141.44 (Bn), 140.83 (C-4), 132.07, 131.72 (C-3 and C-5) (pydc), 131.36 (C_m), 121.27 (C_p), 130.95 (C_o) (Bn), 90.20 (C-4), 85.72 (C-5) (pydc), 45.89 (>CH_2, Bn), 41.39 (C-2), 35.47 (C-8), 28.80 (C-6), 28.64 (C-3), 25.94 (C-7), 18.82 (C-1) (C_8H_{13}). MS (MALDI-TOF, DCTB, CH_2Cl_2): *m*/*z* 467.9 (M^+ − $BnNH_2$).

[Ir(κ^3-pydc)(1-κ-4,5-η-C_8H_{13})(PR_3)]. A solid mixture of [Ir(κ^3-pydc)(1-κ-4,5-η-C_8H_{13})] (**1**·MeOH; 0.100 g, 0.200 mmol) and the corresponding PR_3 (0.200 mmol) was dissolved in CH_2Cl_2/MeOH (3/1, 10 mL), and the solution was stirred at room temperature for 14 h. The resulting solution was evaporated to dryness. The residue was subsequently dissolved in a minimum volume of dichloromethane, and then diethyl ether was added to give the compounds as lemon yellow solids, which were filtered, washed with diethyl ether (3 × 10 mL), and dried under vacuum.

[Ir(κ^3-pydc)(1-κ-4,5-η-C_8H_{13})(PPh_3)] ***(1-PPh_3).*** Yield: 0.137 g (96%). Anal. Found: C, 54.47; H, 4.32; N 1.98. Calcd for $C_{33}H_{31}IrNO_4P$: C, 54.38; H, 4.29; N 1.92. ^{1}H NMR (400.16 MHz, 298 K, CD_2Cl_2): δ 7.81 (t, 1H, J_{H-H} = 8.2 Hz, 4-H), 7.66 (dd, 1H, J_{H-H} = 7.8 and 1.2 Hz), 7.57 (dd, 1H, J_{H-H} = 7.8 and 1.2 Hz) (3-H and 5-H) (pydc), 7.32 (tq, 3H, J_{H-H} = 7.3 and 1.5 Hz), 7.21 (td, 6H, J_{H-H} = 7.3 and 2.0 Hz), 7.13 (tt, 6H, J_{H-H} = 8.3 and 1.3 Hz) (PPh_3), 5.70 (t, 1H, J_{H-H} = 6.8 Hz, 4-H), 5.61 (t, 1H, J_{H-H} = 8.6 Hz, 5-H), 2.95 (d, 1H, J_{H-H} = 16.9 Hz, 6-H), 2.35−2.48 (m, 1H, 3-H), 2.20−2.30 (m, 2H, 3-H and 6-H), 2.11 (m, 1H, 2-H), 1.84 (dtt, 1H, J_{H-H} = 18.1, 13.9, and 4.3 Hz, 7-H), 1.59 (d, 1H, J_{H-H} = 13.9 Hz, 7-H), 1.46 (q, 1H, J_{H-H} = 3.3 Hz, 1-H), 1.34 (td, 1H, J_{H-H} = 3.3 and 13.9 Hz, 8-H), 0.89 (m, 1H, 2-H), 0.65 (m, 1H, 8-H) (C_8H_{13}). ^{13}C{^{1}H} NMR (75.479 MHz, 298 K, CD_2Cl_2): δ 172.07, 171.48 (*C*O), 145.81, 144.63 (C-2 and C-6), 137.56 (C-4) (pydc), 133.77 (d, J_{C-P} = 10.5 Hz, C_o), 130.47 (C_p) (PPh_3), 129.40, 129.10 (C-3 and C-5, pydc), 128.82 (d, J_{C-P} = 8.9 Hz, C_m), 128.63 (d, J_{C-P} = 60.0 Hz, C_{ipso}) (PPh_3), 90.67 (C-4), 82.15 (C-5), 37.59 (d, J_{C-P} = 3.8 Hz), 32.46 (d, J_{C-P} = 3.4 Hz) (C-2 and C-8), 31.72 (d, J_{C-P} = 85.8 Hz, C-1), 27.33 (d, J_{C-P} = 7.2 Hz, C-7), 26.11, 23.39 (C-3 and C-6) (C_8H_{13}). ^{31}P{^{1}H} NMR (161.99 MHz, 298 K, CD_2Cl_2): δ −7.23 (s). MS (MALDI-TOF, DCTB, CH_2Cl_2): *m*/*z* 467.9 (M^+ − PPh_3).

[Ir(κ^3-pydc)(1-κ-4,5-η-C_8H_{13})(PMe_3)] ***(1-PMe_3).*** Yield: 0.098 g (90%). Anal. Found: C, 39.74; H, 4.69; N, 2.54. Calcd for $C_{18}H_{25}IrNO_4P$: C, 39.84; H, 4.64; N 2.58. ^{1}H NMR (400.16 MHz, 298 K, CD_2Cl_2): δ 8.07 (t, 1H, J_{H-H} = 7.5 Hz, 4-H), 8.02 (dd, 1H, J_{H-H} = 9.4 and 1.4 Hz), 7.97 (dd, 1H, J_{H-H} = 9.4 and 1.4 Hz) (3-H and 5-H) (pydc), 5.86 (t, 1H, J_{H-H} = 8.8 Hz, 4-H), 5.55 (t, 1H, J_{H-H} = 8.8 Hz, 5-H), 3.00 (d, 1H, J_{H-H} = 16.9 Hz), 2.53 (m, 1H), 2.25 (m,

dx.doi.org/10.1021/om400767d | *Organometallics* XXXX, XXX, XXX−XXX

1H), 2.15−1.97 (m, 2H), 1.83 (dtt, 1H, J_{H-H} = 13.9, 18.3, and 3.7 Hz), 1.56 (m, 1H), 1.29−1.15 (m, 2H), 0.97 (m, 1H) (C_8H_{13}), 0.87 (d, 9H, J_{H-P} = 14.3 Hz, PMe_3), 0.79 (m, 1H, C_8H_{13}). $^{13}C\{^1H\}$ NMR (100.62 MHz, 298 K, CD_2Cl_2): δ 172.58 (d, J_{C-P} = 2.2 Hz), 172.05 (d, J_{C-P} = 2.9 Hz) (CO), 146.09, 145.13 (C-2 and C-6), 138.34 (d, J_{C-P} = 2.2 Hz, C-4), 129.82 (d, J_{C-P} = 2.2 Hz), 129.46 (t, J = 2.9 Hz) (C-3 and C-5) (pydc), 87.93 (d, J_{C-P} = 1.5 Hz, C-4), 82.44 (C-5), 37.17 (d, J_{C-P} = 4.4 Hz), 32.54 (d, J_{C-P} = 3.7 Hz) (C-2 and C-8), 31.29 (d, J_{C-P} = 91.5 Hz, C-1), 28.42 (d, J_{C-P} = 8.1 Hz, C-7), 26.64, 23.83 (C-3 and C-6) (C_8H_{13}), 9.46 (d, J = 22.0 Hz, PMe_3). $^{31}P\{^1H\}$ NMR (161.99 MHz, 298 K, CD_2Cl_2): δ −38.98 (s). MS (MALDI-TOF, DCTB, CH_2Cl_2): m/z 467.9 ($M^+ - PMe_3$).

[Ir(κ^3-pydc)(1-κ-4,5-η-C_8H_{13})(κ^1-dppm)] (1-dppm). A solution of [Ir(κ^3-pydc)(1-κ-4,5-η-C_8H_{13})] (**1**·MeOH) (0.100 g, 0.200 mmol) in CH_2Cl_2/MeOH (3/1, 10 mL) was slowly cannulated into a solution of dppm (0.077 g, 0.20 mmol) in CH_2Cl_2 (5 mL). The reaction mixture was stirred at room temperature for 14 h and then evaporated to dryness. The residue was dissolved in the minimum volume of dichloromethane, and then diethyl ether was added to give a lemon yellow solid, which was filtered, washed with diethyl ether (3 × 10 mL), and dried under vacuum. Yield: 0.148 g (87%). Crystals suitable for X-ray diffraction were grown by slow diffusion of diethyl ether into a dichloromethane solution of **1-dppm** at 258 K. Anal. Found: C, 56.62; H, 4.32; N, 1.42. Calcd for $C_{40}H_{38}IrNO_4P_2$: C, 56.46; H, 4.50; N, 1.65. ^1H NMR (400.16 MHz, 298 K, CD_2Cl_2): δ 7.65 (td, 1H, J_{H-H} = 7.7 and 1.3 Hz, 4-H), 7.58 (dd, 1H, J_{H-H} = 7.8 and 1.3 Hz), 7.45 (dd, 1H, J_{H-H} = 7.8 and 1.3 Hz) (3-H and 5-H) (pydc), 7.19−7.04 (m, 14H, Ph), 6.99 (m, 2H, Ph), 6.91 (m, 2H, Ph), 6.84 (m, 2H, Ph) (dppm), 6.43 (t, 1H, J_{H-H} = 7.8 Hz, 4-H), 6.16 (t, 1H, J_{H-H} = 8.6 Hz, 5-H), 3.06 (d, 1H, J_{H-H} = 20.0 Hz) (C_8H_{13}), 3.02 (d, 2H, J_{H-H} = 6.8 Hz, >CH_2, dppm), 2.48 (m, 1H), 2.30−2.18 (m, 2H), 2.05 (m, 1H), 1.87 (m, 1H), 1.61 (d, 1H, J_{H-H} = 14.9 Hz), 1.38−1.25 (bm, 2H), 0.88 (m, 1H), 0.65 (m, 1H) (C_8H_{13}). $^{13}C\{^1H\}$ NMR (75.479 MHz, 298 K, CD_2Cl_2): δ 172.30, 171.58 (CO), 145.74 (d, J_{C-P} = 1.6 Hz), 144.30 (d, J_{C-P} = 1.6 Hz) (C-2 and C-6) (pydc), 138.12 (d, J_{C-P} = 32.6 Hz), 138.04 (d, J_{C-P} = 31.2 Hz), 137.94 (d, J_{C-P} = 32.4 Hz), 137.85 (d, J_{C-P} = 30.9 Hz) (C_{ipso}, dppm), 137.15 (d, J_{C-P} = 1.6 Hz, C-4) (pydc), 133.72 (d, J_{C-P} = 10.3 Hz), 133.70 (d, J_{C-P} = 10.4 Hz), 133.07, 132.78, 132.40, 132.27 (d, J_{C-P} = 10.0 Hz), 132.26 (d, J_{C-P} = 9.9 Hz), 132.13 (dppm), 130.44 (d, J_{C-P} = 2.0 Hz), 129.60 (d, J_{C-P} = 2.0 Hz) (C-3 and C-5) (pydc), 129.05, 128.68, 128.56 (d, J_{C-P} = 7.8 Hz), 128.55, 128.40 (d, J_{C-P} = 8.3 Hz), 128.39 (d, J_{C-P} = 8.5 Hz), 128.23 (dppm), 89.64 (d, J_{C-P} = 6.7 Hz, C-4), 81.72 (d, J_{C-P} = 7.8 Hz, C-5) (pydc), 37.09 (d, J_{C-P} = 5.9 Hz), 32.24 (d, J_{C-P} = 3.3 Hz) (C-2 and C-8), 31.57 (d, J_{C-P} = 86.2 Hz, C-1), 27.55 (d, J_{C-P} = 7.3 Hz, C-7), 26.07 (C-3 or C-6) (C_8H_{13}), 23.96 (dd, J_{C-P} = 31.2 and 16.7 Hz, >CH_2, dppm), 23.66 (C-3 or C-6) (C_8H_{13}). $^{31}P\{^1H\}$ NMR (161.99 MHz, 298 K, CD_2Cl_2): δ −17.47 (d, J_{P-P} = 70.7 Hz), −27.81 (d, J_{P-P} = 70.7 Hz). MS (MALDI-TOF, DCTB, CH_2Cl_2): m/z 961.2 [Ir(dppm)$_2^+$], 684.1 (M^+ − pydc).

[Ir(κ^3-pydc)(1-κ-4,5-η-C_8H_{13})]$_2$(μ-diphosphine). A solid mixture of [Ir(κ^3-pydc)(1-κ-4,5-η-C_8H_{13})] (**1**·MeOH; 0.100 g, 0.200 mmol) and the corresponding diphosphine (0.100 mmol) was dissolved in CH_2Cl_2/MeOH (3/1, 10 mL), and the solution was stirred at room temperature for 14 h. The yellow solution was evaporated to dryness to give a yellow solid. The solid was dissolved in the minimum volume of dichloromethane, and then diethyl ether was added. The yellow lemon solid that was obtained was filtered, washed with diethyl ether (3 × 10 mL), and dried under vacuum.

*[Ir(κ^3-pydc)(1-κ-4,5-η-C_8H_{13})]$_2$(μ-dppm) (**1$_2$-dppm**).* Yield: 0.110 g (84%). Anal. Found: C, 49.81; H, 4.23; N, 2.20. Calcd for $C_{55}H_{54}Ir_2N_2O_8P_2$: C, 50.14; H, 4.13; N, 2.13. ^1H NMR (400.16 MHz, 298 K, CD_2Cl_2): δ 7.95−7.82 (m, 2H), 7.71 (d, 1H), 7.66−7.62 (m, 3H) (pydc), 7.21−7.10 (br m, 6H, Ph), 6.98−6.89 (br m, 6H, Ph), 6.80 (m, 4H, Ph), 6.64 (bd, 4H, Ph) (dppm), 5.46 (m, 1H), 5.24 (m, 1H), 5.17 (m, 2H) (=CH, C_8H_{13}), 2.83 (m, 2H), 2.36 (m, 2H), 2.27−1.98 (set of m, 6H), 1.77 (m, 2H), 1.59 (set of m, 4H), 1.34 (m, 2H), 1.19 (m, 2H), 0.80 (m, 2H), 0.57 (m, 2H) (>CH_2, C_8H_{13} and dppm). $^{31}P\{1H\}$ NMR (161.99 MHz, 298 K, CD_2Cl_2): δ −10.96 (s), −11.64 (s). MS (MALDI-TOF, DCTB, CH_2Cl_2): m/z 961.2 [Ir(dppm)$_2^+$]. MS (ESI, CH_3CN): m/z 850.2 (M^+ − **1**).

*[Ir(κ^3-pydc)(1-κ-4,5-η-C_8H_{13})]$_2$(μ-dppe) (**1$_2$-dppe**).* Yield: 0.113 g (85%). Anal. Found: C, 50.39; H, 3.98; N, 2.01. Calcd for $C_{56}H_{56}Ir_2N_2O_8P_2$: C, 50.52; H, 4.24; N, 2.10. ^1H NMR (400.16 MHz, 298 K, CD_2Cl_2): δ 7.81 (t, 1H, J_{H-H} = 7.8 Hz), 7.79 (t, 1H, J_{H-H} = 7.8 Hz), 7.69 (dd, 1H, J_{H-H} = 7.8 and 1.3 Hz), 7.60 (dd, 1H, J_{H-H} = 7.8 and 1.3 Hz), 7.57 (dd, 1H, J_{H-H} = 7.8 and 1.3 Hz), 7.50 (dd, 1H, J_{H-H} = 7.8 and 1.3 Hz) (pydc), 7.40−7.10 (set of m, 12H), 6.97 (t, 2H, J_{H-H} = 8.4 Hz), 6.87 (m, 4H), 6.79 (t, 2H, J_{H-H} = 8.1 Hz) (Ph, dppe), 5.76 (t, 1H, J_{H-H} = 8.8 and 2.8 Hz), 5.66 (br m, 3H) (=CH, C_8H_{13}), 2.99 (d, 2H, J = 16.2 Hz), 2.43 (m, 2H), 2.13 (m, 4H), 2.0 (m, 2H), 1.90−1.65 (set of m, 6H), 1.59 (m, 2H), 1.35−1.15 (m, 4H), 0.80 (m, 2H), 0.63 (m, 2H) (>CH_2, C_8H_{13} and dppe). $^{13}C\{^1H\}$ NMR (100.63 MHz, 298 K, CD_2Cl_2): δ 171.18, 172.14, 171.63, 171.56 (CO), 145.72, 144.58 (C-2 and C-6), 138.16, 138.07 (C-4) (pydc), 133.0−132.23, 131.05, 130.91, 130.79, 130.60, 129.69−129.47 (Ph, dppe), 129.47, 129.40, 129.19, 129.12 (C-3 and C-5, pydc), 127.50−126.66 (C_{ipso}, Ph, dppe), 90.13, 89.45, 82.06, 81.45 (C-4 and C-5, C_8H_{13}), 37.47, 37.26 (>CH_2), 32.55 (dd, J_{C-P} = 90.0 and 2.2 Hz, C-1), 32.56, 32.39 (>CH_2), 32.41 (dd, J_{C-P} = 90.0 and 2.2 Hz, C-1) (C_8H_{13}), 27.89 (t, J_{C-P} = 3.6 Hz, >CH_2), 27.73 (t, J_{C-P} = 3.6 Hz, >CH_2) (dppe), 26.43, 26.33, 23.51, 23.49, 17.04 (d, J_{C-P} = 7.3 Hz), 16.79 (d, J_{C-P} = 6.6 Hz) (>CH_2, C_8H_{13}). $^{31}P\{^1H\}$ NMR (161.99 MHz, 298 K, CD_2Cl_2): δ −13.68 (s), −13.82 (s). MS (MALDI-TOF, DCTB, CH_2Cl_2): m/z 989.2 [Ir(dppe)$_2^+$], 699.1 [Ir(C_8H_{13})(dppe)$^+$]. MS (ESI, CH_3CN): m/z 1329.2 $[M]^+$, 864.2 (M^+ − **1**).

*[Ir(κ^3-pydc)(1-κ-4,5-η-C_8H_{13})]$_2$(μ-dppp) (**1$_2$-dppp**).* Yield: 0.112 g (83%). Anal. Found: C, 50.45; H, 4.31; N, 2.21. Calcd for $C_{57}H_{58}Ir_2N_2O_8P_2$: C, 50.88; H, 4.34; N, 2.08. ^1H NMR (400.16 MHz, 298 K, CD_2Cl_2): δ 7.73 (t, 1H, J_{H-H} = 7.6 Hz,), 7.72 (t, 1H, J_{H-H} = 7.6 Hz) (4-H, pydc), 7.64 (dd, 1H, J_{H-H} = 7.8 and 1.3 Hz), 7.59 (dd, 1H, J_{H-H} = 7.6 and 1.3 Hz), 7.46 (br d, 1H, J_{H-H} = 7.6 Hz), 7.41 (br d, 1H, J_{H-H} = 7.3 Hz) (H-3 and H-5, pydc), 7.28 (t, 2H, J_{H-H} = 7.3 Hz,), 7.19−7.13 (set of m, 6H), 7.11−7.01 (set of m, 8H), 6.91 (t, 2H, J_{H-H} = 8.32 Hz), 6.79 (t, 2H, J_{H-H} = 8.4 Hz) (Ph, dppp), 5.77 (m, 2H), 5.66 (br t, 1H, J_{H-H} = 8.4 Hz), 5.58 (t, 1H, J_{H-H} = 8.4 Hz) (H-4 and H-5, pydc), 2.88 (d, 1H, J_{H-H} = 16.7 Hz), 2.79 (d, 1H, J_{H-H} = 16.2 Hz), 2.42−2.37 (m, 3H), 2.28−2.10 (m, 6H), 2.05−1.90 (m, 4H), 1.88−1.70 (m, 3H), 1.51 (t, 2H, J_{H-H} = 12.1 Hz), 1.27 (m, 4 H), 0.91−0.82 (m, 2H), 0.67−0.57 (m, 2H) (>CH_2, dppp and C_8H_{13}). $^{31}P\{^1H\}$ NMR (161.99 MHz, 298 K, CD_2Cl_2): δ −17.12 (s), −18.10 (s). MS (ESI, CH_3CN): m/z 879.2 (M^+ − **1**).

Theoretical Calculations. All computations were performed using the Gaussian 09 (RevB.01) package.[46] The structures were fully optimized without geometrical constraints, and the stationary points (minima and TS) were confirmed by frequency calculations. The connections between the transition states and the minima were checked by visual inspection of the negative frequency, and an extensive IRC calculation in both directions was performed for the transition state $TS_{4\text{-}4c}$. The calculations were carried out using the B3LYP functional, and the basis sets used were LANL2DZ supplemented with an f function and its associated ECP for iridium[47] and 6-31G** for the rest of the atoms. Solution calculations were performed in dichloromethane as solvent using the SMD continuum model as implemented in Gaussian 09. Gas-phase energies are reported as Gibbs energies and solution phase energies as E (solv, CH_2Cl_2, SMD). The structures of the optimized molecules were depicted with the CyLview program.[48]

Crystal Structure Determination. Data collection was performed at low temperature (100(2) K) on a Bruker SMART APEX CCD (**1-py** and **1-dppm**) or on a Bruker APEX DUO (**7**) diffractometer equipped with graphite-monochromated Mo Kα radiation (λ = 0.71073 Å) using narrow frames (0.3° in ω). Cell parameters were refined from the observed setting angles and detector positions of strong reflections (31744 reflections, $2\theta \leq 30.27°$ (**7**); 9435 reflections, $2\theta \leq 28.85°$ (**1-py**); 894 reflections, $2\theta \leq 16.57°$ (**1-dppm**)). Data were corrected for Lorentz and polarization effects using SAINT-PLUS,[49] and a multiscan absorption correction was applied with the SADABS program.[50] The structure was solved by Patterson or direct methods and completed by successive difference Fourier syntheses (SHELXS-86).[51] Refinement was carried out by full-

dx.doi.org/10.1021/om400767d | Organometallics XXXX, XXX, XXX−XXX

matrix least squares on F^2 with SHELXL97,[52] including isotropic and subsequent anisotropic displacement parameters for all non-hydrogen atoms. Treatment of hydrogen atoms and detected static disorder problems are described below.

Crystal data for ***1-py****:* $C_{20}H_{21}IrN_2O_4$, M_r = 545.59, monoclinic, space group $P2_1/n$, crystal size 0.221 × 0.203 × 0.023 mm, a = 9.6334(6) Å, b = 15.3382(9) Å, c = 13.2311(8) Å, β = 111.1380(10)°, V = 1823.47(19) Å^3, Z = 4, ρ_{calcd} = 1.987 g cm^{-3}, μ(Mo Kα) = 7.351 mm^{-1}, minimum and maximum transmission factors 0.293 and 0.849, 22260 measured reflections ($2.12 \leq \theta \leq 28.86°$), 4476 unique reflections (R_{int} = 0.0409); 4476/0/327 data/restraints/parameters, final R1 = 0.0276 ($I > 2\sigma(I)$), wR2 = 0.06373, S = 1.066 for all data; maximum difference peak/hole 1.972/−1.383 e Å^{-3}. Hydrogen atoms of the carboxylate and pyridine ligands were included in observed positions and refined as free isotropic atoms. Anomalous displacement parameters revealed the presence of static disorder involving five carbon atoms of the σ,π-cyclooctenyl ligand. Two fragments with complementary occupancies were included in the refinement. Carbon atoms with the lower occupancy were maintained isotropic, whereas those of higher occupancy were refined anisotropically. Hydrogen atoms were included in calculated positions for this disordered ligand.

Crystal data for ***1-dppm****:* $C_{40}H_{38}IrNO_4P_2$, M_r = 850.85, triclinic, space group $P\bar{1}$, crystal size 0.081 × 0.049 × 0.018 mm, a = 9.6225(13) Å, b = 13.0524(17) Å, c = 15.245(2) Å, α = 111.006(3)°, β = 95.558(3)°, γ = 103.966(3)°, V = 1698.8(4) Å^3, Z = 2, ρ_{calcd} = 1.663 g cm^{-3}, μ(Mo Kα) = 4.068 mm^{-1}, minimum and maximum transmission factors 0.734 and 0.930, 18343 measured reflections ($1.75 \leq \theta \leq 25.68°$), 6428 unique reflections (R_{int} = 0.1020), 6428/0/450 data/restraints/parameters; final R1 = 0.0618 ($I > 2\sigma(I)$), wR2 = 0.1071, S = 1.032 for all data; maximum difference peak/hole 1.107/−2.072 e Å^{-3}. Hydrogens were introduced in calculated positions and refined with positional and displacement riding parameters. An analogous static disorder of the σ,π-cyclooctenyl ligand to that described for **1-py** was observed. A similar model based on two partial fragments was established for this molecule.

Crystal data for ***7****:* $C_{84}H_{130}Ir_4N_2O_8{\cdot}2CH_3OH$, M_r = 2128.78, tetragonal, space group $P4_2/n$, crystal size 0.329 × 0.127 × 0.096 mm, a = 16.7340(7) Å, b = 19.659(2) Å, c = 28.8823(12) Å, β = 106.824(2)°, V = 8087.8(6) Å^3, Z = 4, ρ_{calcd} = 1.748 g cm^{-3}, μ(Mo Kα) = 6.619 mm^{-1}, minimum and maximum transmission factors 0.242 and 0.428, 94357 measured reflections ($1.72 \leq \theta \leq 30.53°$), 11887 unique reflections (R_{int} = 0.0323), 11887/0/716 data/restraints/parameters; final R1 = 0.0256 ($I > 2\sigma(I)$), wR2 = 0.0713, S = 1.069 for all data; maximum difference peak/hole 1.870/−0.521 e Å^{-3}. Most of the hydrogen atoms of the metal cluster were observed in the difference Fourier maps and refined as free isotropic atoms. A methanol solvent molecule was highly disordered among the metal complexes; two independent CO moieties (without hydrogen atoms) with complementary occupancy factors were included in the model to account for the presence of this solvent.

■ ASSOCIATED CONTENT

Ⓢ Supporting Information

CIF files giving X-ray crystallographic data for the structure determinations of compounds **1-py**, **1-dppm**, and **7**, tables giving optimized coordinates for compounds **1** and **4**, species **4a**−**e**, and related transition states, and an animation of the methanol-assisted proton transfer process. This material is available free of charge via the Internet at http://pubs.acs.org.

■ AUTHOR INFORMATION

Corresponding Author

*J.J.P.-T.: e-mail, perez@unizar.es; fax, 34 976761143; tel, 34 976762025.

Notes

The authors declare no competing financial interest.

■ ACKNOWLEDGMENTS

Financial support from the Ministerio de Economía y Competitividad (MEC/FEDER) of Spain (Project CTQ2010-15221), Diputación General de Aragón (Group E07) and Fondo Social Europeo, and CONSOLIDER INGENIO-2010, under the Projects MULTICAT (CSD2009-00050) and Factoría de Crystalización (CSD2006-0015), is gratefully acknowledged. I.G. thanks the Humboldt Foundation for a research fellowship. We also thank Centro de Supercomputación de Galicia (CESGA) for access to their computational facilities. This paper is dedicated to Professor Antonio Laguna on the occasion of his 65th birthday.

■ REFERENCES

(1) (a) Choi, J.; MacArthur, A. H. R.; Brookhart, M.; Goldman, A. S. *Chem. Rev.* **2011**, *111*, 1761−1779. (b) Selander, N.; Szabó, K. J. *Chem. Rev.* **2011**, *111*, 2048−2076. (c) Leisa, W.; Mayera, H. A.; Kaska, W. C. *Coord. Chem. Rev.* **2008**, *252*, 1787−1797. (d) Albrecht, M.; van Koten, G. *Angew. Chem., Int. Ed.* **2001**, *40*, 3750−3781.

(2) *The Chemistry of Pincer Compounds*; Morales-Morales, D., Jensen, C. M., Eds.; Elsevier: Amsterdam, 2007.

(3) (a) Romain, C.; Brelot, L.; Bellemin-Laponnaz, S.; Dagorne, S. *Organometallics* **2010**, *29*, 1191−1198. (b) Klein, A.; Elmas, S.; Butsch, K. *Eur. J. Inorg. Chem.* **2009**, 2271−2281. (d) Agapie, T.; Day, M. W.; Bercaw, J. E. *Organometallics* **2008**, *27*, 6123−6142. (c) Agapie, T.; Henling, L. H.; DiPasquale, A. G.; Rheingold, A. L.; Bercaw, J. E. *Organometallics* **2008**, *27*, 6245−6256.

(4) (a) O'Reilly, M. E.; Ghiviriga, I.; Abboud, K. A.; Veige, A. S. *J. Am. Chem. Soc.* **2012**, *134*, 11185−11195. (b) Sarkar, S.; McGowan, K. P.; Kuppuswamy, S.; Ghiviriga, I.; Abboud, K. A.; Veige, A. S. *J. Am. Chem. Soc.* **2012**, *134*, 4509−4512. (c) O'Reilly, M. E.; Del Castillo, T. J.; Abboud, K. A.; Veige, A. S. *Dalton Trans.* **2012**, *41*, 2237−2246. (d) Kuppuswamy, S.; Peloquin, A. J.; Ghiviriga, I.; Abboud, K. A.; Veige, A. S. *Organometallics* **2010**, *29*, 4227−4233.

(5) (a) Szigethy, G.; Heyduk, A. F. *Dalton Trans.* **2012**, *41*, 8144−8152. (b) Lu, F.; Zarkesh, R. A.; Heyduk, A. F. *Eur. J. Inorg. Chem.* **2012**, 467−470. (c) Heyduk, A. F.; Zarkesh, R. A.; Nguyen, A. I. *Inorg. Chem.* **2011**, *50*, 9849−9863. (d) Zarkesh, R. A.; Heyduk, A. F. *Organometallics* **2011**, *30*, 4890−4898.

(6) (a) Hartwig, J. F. *Acc. Chem. Res.* **2012**, *45*, 864−873. (b) Mkhalid, I. A. I.; Barnard, J. H.; Marder, T. B.; Murphy, J. M.; Hartwig, J. F. *Chem. Rev.* **2010**, *110*, 890−931. (c) *Activation and Functionalization of C-H Bonds*; Goldberg, K. I., Goldman, A. S., Eds.; American Chemical Society: Washington, DC, 2004; ACS Symposium Series *885*. (d) Arndtsen, B. A.; Bergman, R. G.; Mobley, T. A.; Peterson, T. H. *Acc. Chem. Res.* **1995**, *28*, 154−162.

(7) (a) Hashiguchi, B. G.; Bischof, S. M.; Konnick, M. M.; Periana, R. A. *Acc. Chem. Res.* **2012**, *45*, 886−898. (b) Bhalla, G.; Periana, R. A. *Angew. Chem., Int. Ed.* **2005**, *44*, 1540−1543. (c) Wong-Foy, A. G.; Bhalla, G.; Lui, X. Y.; Periana, R. A. *J. Am. Chem. Soc.* **2003**, *125*, 14292−14293. (d) Matsumoto, T.; Taube, D. J.; Periana, R. A.; Taube, H.; Yoshida, H. *J. Am. Chem. Soc.* **2000**, *122*, 7414−7415.

(8) Bhalla, G.; Lui, X. Y.; Oxgaard, J.; Goddard, W. A.; Periana, R. A. *J. Am. Chem. Soc.* **2005**, *127*, 11372−11389.

(9) Weinberg, D. R.; Hazari, N.; Labinger, J. A.; Bercaw, J. E. *Organometallics* **2010**, *29*, 89−100.

(10) Fu, R.; Bercaw, J. E.; Labinger, J. A. *Organometallics* **2011**, *30*, 6751−6765.

(11) Nguyen, D. H.; Pérez-Torrente, J. J.; Lomba, L.; Jiménez, M. V.; Lahoz, F. J.; Oro, L. A. *Dalton Trans.* **2011**, *40*, 8429−8435.

(12) (a) Sengupta, S. K.; Sahni, S. K.; Kapoor, R. N. *Polyhedron* **1983**, *2*, 317−322. (b) Matthews, R. W.; Hamer, A. D.; Hoof, D. L.; Tisley, D. G.; Walton, R. A. *Dalton Trans.* **1973**, *10*, 1035−1038.

(13) Some examples of iridium σ,π-cyclooctenyl complexes: (a) Pontiggia, A. J.; Chaplin, A. B.; Weller, A. S. *J. Organomet. Chem.* **2011**, *696*, 2870−2876. (b) Safronov, A. V.; Zinevich, T. V.; Dolgushin, F. M.; Tok, O. L.; Vorontsov, E. V.; Chizhevsky, I. T.

Organometallics **2004**, *23*, 4970−4979. (c) Martin, M.; Sola, E.; Torres, O.; Plou, P.; Oro, L. A. *Organometallics* **2003**, *22*, 5406−5417. (d) Mønsted, L.; Mønsted, O.; Schäffer, S.; Simonsen, K.; Søtofte, I. *Acta Chem. Scand.* **1996**, *50*, 973−978. (e) Esteruelas, M. A.; Olivan, M.; Oro, L. A.; Schulz, M.; Sola, E.; Werner, H. *Organometallics* **1992**, *11*, 3659−36664.

(14) (a) Yamagata, T.; Tadaoka, H.; Nagata, M.; Hirao, T.; Kataoka, Y.; Ratovelomanana-Vidal, V.; Genet, J. P.; Mashima, K. *Organometallics* **2006**, *25*, 2505−2513. (b) Ladipo, F. T.; Kooti, M.; Merola, J. S. *Inorg. Chem.* **1993**, *32*, 1681−1688. (c) van Doorn, J. A.; Masters, C.; van der Woude, C. *J. Chem. Soc., Dalton Trans.* **1978**, 1213−1220.

(15) Elliott, P. I. P.; Haslam, C. E.; Spey, S. E.; Haynes, A. *Inorg. Chem.* **2006**, *45*, 6269−6275.

(16) Åkermark, B.; Martin, J.; Nyström, J.-E.; Strömberg, S.; Svensson, M.; Zetterberg, K.; Zuber, M. *Organometallics* **1998**, *17*, 5367−5373.

(17) (a) Macchioni, A.; Bellachioma, G.; Cardaci, G.; Travaglia, M.; Zuccaccia, C.; Milani, B.; Corso, G.; Zangrando, E.; Mestroni, G.; Carfagna, C.; Formica, M. *Organometallics* **1999**, *18*, 3061−3069. (b) Hoel, G. R.; Stockland, R. A., Jr.; Anderson, G. K.; Ladipo, F. T.; Braddock-Wilking, J.; Rath, N. P.; Mareque-Rivas, J. C. *Organometallics* **1998**, *17*, 1155−1165.

(18) Su, Y.; Song, G.; Han, K.; Li, X. *J. Organomet. Chem.* **2011**, *696*, 1640−1646.

(19) Wang, W.-H.; Muckerman, J. T.; Fujita, E.; Himeda, Y. *ACS Catal.* **2013**, *3*, 856−860.

(20) Jiménez-Tenorio, M.; Puerta, M. C.; Valerga, P.; Ortuño, M. A.; Ujaque, G.; Lledos, A. *Inorg. Chem.* **2013**, *52*, 8919−8932.

(21) Kovacs, G.; Lledos, A.; Ujaque, G. *Organometallics* **2010**, *29*, 3252−3260.

(22) Campos, J.; Espada, M. F.; López-Serrano, J.; Carmona, E. *Inorg. Chem.* **2013**, *52*, 6694−6704.

(23) (a) Ariafard, A.; Asadollah, E.; Ostadebrahim, M.; Rajabi, N. A.; Yates, B. F. *J. Am. Chem. Soc.* **2012**, *134*, 16882−16890. (b) Kovács, G.; Lledós, A.; Ujaque, G. *Organometallics* **2010**, *29*, 5919−5926. (c) Zhang, J.; Shen, W.; Li, L.; Li, M. *Organometallics* **2009**, *28*, 3129−3139. (d) Paton, R. S.; Maseras, F. *Org. Lett.* **2009**, *11*, 2237−2240. (e) Comas-Vives, A.; González-Arellano, C.; Corma, A.; Iglesias, M.; Sánchez, F.; Ujaque, G. *J. Am. Chem. Soc.* **2006**, *128*, 4756−4765.

(24) (a) Zangl, A.; Klufers, P.; Schaniel, D.; Woike, T. *Dalton Trans.* **2009**, 1034−1045. (b) Takuma, M.; Ohki, Y.; Tatsumi, K. *Organometallics* **2005**, *24*, 1344−1347. (c) Suh, I.-H.; Lee, J.-H.; Song, J.-H.; Oh, M.-R.; Suh, J.-S.; Park, S.-J.; Lee, K.-W. *J. Korean Phys. Soc.* **1996**, *29*, 739−744.

(25) (a) Dominguez-Martin, A.; Choquesillo-Lazarte, D.; Gonzalez-Perez, J. M.; Castineiras, A.; Niclos-Gutierrez, J. *J. Inorg. Biochem.* **2011**, *105*, 1073−1080. (b) Meier, R.; Molinier, M.; Anson, C.; Powell, A. K.; Kallies, B.; van Eldik, R. *Dalton Trans.* **2006**, 5506−5514.

(26) Khokhar, R.; Xu, Q.; Al-Baker, S.; Bear, J. L. *Inorg. Chim. Acta* **1992**, *194*, 243−246.

(27) (a) Alonso, P. J.; Benedí, O.; Fabra, M. J.; Lahoz, F. J.; Oro, L. A.; Pérez-Torrente, J. J. *Inorg. Chem.* **2009**, *48*, 7984−7993. (b) Rodman, G. S.; Mann, K. R. *Inorg. Chem.* **1988**, *27*, 3338−3346.

(28) Bombi, G. G.; Aikebaier, R.; Dean, A.; Di Marco, V. B.; Marton, D.; Tapparo, A. *Polyhedron* **2009**, *28*, 327−335.

(29) Mirti, P.; Gennaro, M. C. *J. Inorg. Nucl. Chem.* **1977**, *39*, 1259−1264.

(30) Schwarzenbach, G.; Anderegg, G.; Schneider, W.; Senn, H. *Helv. Chim. Acta* **1955**, *38*, 1147−1171.

(31) Alley, W. M.; Girard, C. W.; Ozkar, S.; Finke, R. G. *Inorg. Chem.* **2009**, *48*, 1114−1121.

(32) Feldman, J.; Calabrese, J. C. *Inorg. Chem.* **1994**, *33*, 5955−5956.

(33) (a) Böttcher, H. C.; Graf, M.; Mayer, P.; Sunkel, K.; Kruger, H. *Inorg. Chim. Acta* **2011**, *365*, 103−107. (b) Geier, M. J.; Vogels, C. M.; Decken, A.; Westcott, S. A. *Eur. J. Inorg. Chem.* **2010**, 4602−4610. (c) Cheung, W.-M.; Lai, C.-Y.; Zhang, Q.-F.; Wong, W.-Y.; Williams, I. D.; Leung, W.-H. *Inorg. Chim. Acta* **2006**, *359*, 2712−2720.

(34) Allen, F. H.; Kennard, O.; Watson, D. G.; Brammer, L.; Orpen, A. G.; Taylor, R. *J. Chem. Soc., Perkin Trans.* **1987**, S1−S19.

(35) Bhalla, G.; Oxgaard, J.; Goddard, W. A., III; Periana, R. A. *Organometallics* **2005**, *24*, 5499−5502.

(36) Atkinson, K. D.; Cowley, M. J.; Elliot, P. I. P.; Duckett, S. B.; Green, G. G. R.; López-Serrano, J.; Whitwood, A. C. *J. Am. Chem. Soc.* **2009**, *131*, 13362−13368.

(37) Kanematsu, N.; Ebihara, M.; Kawamura, T. *J. Chem. Soc., Dalton Trans.* **1999**, 4413−4417.

(38) Data obtained from a specific search on the CSD: Allen, F. H. *Acta Crystallogr.* **2002**, *B58*, 380−388.

(39) (a) Nabavizadeh, S. M.; Haghighi, M. G.; Esmaeilbeig, A. R.; Raoof, F.; Mandegani, Z.; Jamali, S.; Rashidi, M.; Puddephatt, R. J. *Organometallics* **2010**, *29*, 4893−4899. (b) Martínez, J.; Adrio, L. A.; Antelo, J. M.; Ortigueira, J. M.; Pereira, M. T.; Fernández, J. J.; Fernández, A.; Vila, J. M. *J. Organomet. Chem.* **2006**, *691*, 2721−2733. (c) Cadierno, V.; García-Garrido, S. E.; Gimeno, J. *Inorg. Chim. Acta* **2003**, *347*, 41−48.

(40) Alaimo, P. J.; Bergman, R. G. *Organometallics* **1999**, *18*, 2707−2717.

(41) Chaplin, B.; Scopelliti, R.; Dyson, P. J. *Eur. J. Inor. Chem.* **2005**, 4762−4774.

(42) Uson, R.; Oro, L. A.; Cabeza, J. A. *Inorg. Synth.* **1985**, *23*, 126−130.

(43) Ortmann, D. A.; Werner, H. *Z. Anorg. Allg. Chem.* **2002**, *628*, 1373−1376.

(44) Green, M.; Kuc, T. A.; Taylor, S. H. *J. Chem. Soc. A* **1971**, 2334−2337.

(45) Nishiyama, H.; Yamaguchi, M.; Kondo, M.; Itoh, K. *J. Org. Chem.* **1992**, *57*, 4306−4309.

(46) Frisch, M. J.; Trucks, G. W.; Schlegel, H. B.; Scuseria, G. E.; Robb, M. A.; Cheeseman, J. R.; Scalmani, G.; Barone, V.; Mennucci, B.; Petersson, G. A.; Nakatsuji, H.; Caricato, M.; Li, X.; Hratchian, H. P.; Izmaylov, A. F.; Bloino, J.; Zheng, G.; Sonnenberg, J. L.; Hada, M.; Ehara, M.; Toyota, K.; Fukuda, R.; Hasegawa, J.; Ishida, M.; Nakajima, T.; Honda, Y.; Kitao, O.; Nakai, H.; Vreven, T.; Montgomery, J. A.; Peralta, J. E.; Ogliaro, F.; Bearpark, M.; Heyd, J. J.; Brothers, E.; Kudin, K. N.; Staroverov, V. N.; Kobayashi, R.; Normand, J.; Raghavachari, K.; Rendell, A.; Burant, J. C.; Iyengar, S. S.; Tomasi, J.; Cossi, M.; Rega, N.; Millam, J. M.; Klene, M.; Knox, J. E.; Cross, J. B.; Bakken, V.; Adamo, C.; Jaramillo, J.; Gomperts, R.; Stratmann, R. E.; Yazyev, O.; Austin, A. J.; Cammi, R.; Pomelli, C.; Ochterski, J. W.; Martin, R. L.; Morokuma, K.; Zakrzewski, V. G.; Voth, G. A.; Salvador, P.; Dannenberg, J. J.; Dapprich, S.; Daniels, A. D.; Farkas, Ö.; Foresman, J. B.; Ortiz, J. V.; Cioslowski, J.; Fox, D. J. *Gaussian 09, Revision B.01*; Gaussian Inc., Wallingford, CT, 2009.

(47) Ehlers, A.; Böhme, M.; Dapprich, S.; Gobbi, A.; Höllwarth, A.; Jonas, V.; Köhler, K.; Stegmann, R.; Veldkamp, A.; Frenking, G. *Chem. Phys. Lett.* **1993**, *208*, 111−114.

(48) Legault, C. Y. *CyLview*, Université de Sherbrooke, Sherbrooke, Canada, 2009.

(49) *SAINT-PLUS, version 6.01*; Bruker AXS, Inc, Madison, WI, USA, 2001.

(50) *SADABS, Area-Detector Absorption Correction Program*; Bruker-AXS, Inc., Madison, WI, USA, 2001.

(51) (a) Sheldrick, G. M. *Acta Crystallogr.* **1990**, *A46*, 467−473. (b) Sheldrick, G. M. *Methods Enzymol.* **1997**, *276*, 628−641.

(52) (a) Sheldrick, G. M. *SHELXL-97, A Program for Crystal Structure Refinement*; University of Göttingen, Göttingen, Germany, 1997. (b) Sheldrick, G. M. *Acta Crystallogr. Sect. A: Fundam. Crystallogr.* **2008**, *64*, 112−122.